

AEDC-TR-69-156

cy 1

**ARCHIVE COPY  
DO NOT LOAN**

PROPERTY OF U. S. AIR FORCE  
AEDC LIBRARY  
24700-69-0001



**NUMERICAL STUDY OF  
THE EARLY POPULATION DENSITY  
RELAXATION OF THERMAL HYDROGEN PLASMAS**

**C. C. Limbaugh and W. K. McGregor, Jr.**

**ARO, Inc.  
and**

**A. A. Mason**

**The University of Tennessee Space Institute**

**October 1969**

This document has been approved for public release  
and sale; its distribution is unlimited.

**ROCKET TEST FACILITY**

**ARNOLD ENGINEERING DEVELOPMENT CENTER**

**AIR FORCE SYSTEMS COMMAND**

**ARNOLD AIR FORCE STATION, TENNESSEE**

PROPERTY OF U. S. AIR FORCE  
AEDC LIBRARY  
F40600-69-C-0001

AEDC TECHNICAL LIBRARY



5 0720 00032 0178

# *NOTICES*

When U. S. Government drawings, specifications, or other data are used for any purpose other than a definitely related Government procurement operation, the Government thereby incurs no responsibility nor any obligation whatsoever, and the fact that the Government may have formulated, furnished, or in any way supplied the said drawings, specifications, or other data, is not to be regarded by implication or otherwise, or in any manner licensing the holder or any other person or corporation, or conveying any rights or permission to manufacture, use, or sell any patented invention that may in any way be related thereto.

Qualified users may obtain copies of this report from the Defense Documentation Center.

References to named commercial products in this report are not to be considered in any sense as an endorsement of the product by the United States Air Force or the Government.

NUMERICAL STUDY OF  
THE EARLY POPULATION DENSITY  
RELAXATION OF THERMAL HYDROGEN PLASMAS

C. C. Limbaugh and W. K. McGregor, Jr.  
ARO, Inc.  
and  
A. A. Mason  
The University of Tennessee Space Institute

This document has been approved for public release  
and sale; its distribution is unlimited.

## FOREWORD

The work reported herein was sponsored by the Arnold Engineering Development Center (AEDC), Air Force Systems Command (AFSC), Arnold Air Force Station, Tennessee, under Program Element 61102F, Project 8951, Task 05.

The research was conducted by ARO, Inc. (a subsidiary of Sverdrup & Parcel and Associates, Inc.), contract operator of AEDC, AFSC, under Contract No. F40600-69-C-0001. The work reported is part of a continuing study under ARO Project No. RW5910 in the Research Branch of the Rocket Test Facility (RTF) and covers research efforts from July 1, 1968 to March 1, 1969. The manuscript was submitted for publication on June 13, 1969.

This technical report has been reviewed and is approved.

Michael G. Buja  
2nd Lt, USAF  
Research Division  
Directorate of Plans  
and Technology

Harry L. Maynard  
Colonel, USAF  
Director of Plans  
and Technology

## ABSTRACT

The purpose of this investigation was to examine the early relaxation of the population density distribution of a thermal hydrogen plasma. The system of rate equations describing the transient behavior of all quantum levels was used and solved numerically. Three hypothetical hydrogen plasmas were studied, each with an excitation temperature of 10,000°K. Two of the plasmas differed only by the transition probability of the quasi-metastable ( $2S_{1/2}$ ) eigenstate, whereas the third case used a different initial population density distribution. The plasmas were used to study the fundamental consistency of the mathematical model, the existence and location of the critical level, relaxation to the quasi-steady state, and a quantitative study of the effects of the quasi-metastable level on the excited state population density distribution. The results show that the model is consistent with fundamental theory under strong collision dominance and that the critical level does exist at that level predicted by earlier investigators. The quasi-metastable state has a significant effect on the excited state population density distribution, and a simple dual-based Maxwell-Boltzmann distribution is shown to accurately predict the results. The computations involved terminate at a real plasma time of  $1 \times 10^{-5}$  sec.

## CONTENTS

	<u>Page</u>
ABSTRACT . . . . .	iii
I. INTRODUCTION . . . . .	1
II. MODEL	
2.1 Theoretical Model . . . . .	4
2.2 Reduction of the Theoretical Model . . . . .	8
2.3 Collisional-Radiative Recombination Model . . . . .	8
2.4 Critical Level . . . . .	9
2.5 Dual-Based Maxwell-Boltzmann Distribution . . . . .	10
III. RATE COEFFICIENTS	
3.1 Einstein Probabilities, $A(p, q)$ . . . . .	11
3.2 Radiative Recombination, $\beta(p)$ . . . . .	11
3.3 Collisional Rate Coefficients, $K(p, q)$ , $K(p, c)$ , $K(c, p)$ . . . . .	12
3.4 Discussion of Rate Coefficients . . . . .	14
IV. NUMERICAL ANALYSIS	
4.1 Theory . . . . .	15
4.2 Application . . . . .	16
4.3 Extrapolations . . . . .	17
4.4 Reporting of Data . . . . .	18
V. RESULTS OF COMPUTATIONS	
5.1 Fundamental Consistency . . . . .	19
5.2 Critical Level . . . . .	20
5.3 Number Density Distribution and Rates . . . . .	21
5.4 Time Comparison of Metastable and Nonmetastable Cases . . . . .	23
5.5 Dual-Based Maxwell-Boltzmann Distribution . . . . .	26
5.6 Convergence to the CRR Model . . . . .	27
VI. CONCLUDING REMARKS . . . . .	28
REFERENCES . . . . .	30

## APPENDIXES

## I. ILLUSTRATIONS

Figure

1. Time Development of the Test Cases . . . . .	35
2. Comparison of Time Developments of Quantum Level 3 . . . . .	36

<u>Figure</u>	<u>Page</u>
3. Comparison of Time Developments of Quantum Level 5 . . . . .	37
4. Comparison of Time Developments of Quantum Level 10 . . . . .	38
5. Comparison of Time Developments of Continuum Densities . . . . .	39
6. Time Development of the (2, 0) Population Densities . . . . .	40
7. Time Development of Quantum Level 5 . . . . .	41
8. Boltzmann Plot of Metastable Case A at Various Times . . . . .	42
9. Comparison of the Eigenstate Rate Equations Solution with the Dual-Based Maxwell-Boltzmann Distribution . . . . .	43

II. TABLES

I. Radiative Recombination Coefficient, $\beta(p)$ . . . . .	44
II. Two-Body Ionization Coefficient, $K(p, c)$ . . . . .	44
III. Three-Body Recombination Coefficient, $\frac{K(c, p)}{n_c}$ . . . . .	45
IV. Two-Body Internal Transition Coefficient, $K(p, q)$ . . . . .	46
V. Time at Which Saha Equilibrium Is Established, Case A . . . . .	47
VI. Initial and Final Population Density Distribution, Case A . . . . .	48
VII. Initial and Final Population Density Distribution, Case B . . . . .	49
VIII. Detailed Rates at $1 \times 10^{-15}$ sec . . . . .	50
IX. Detailed Rates at $5 \times 10^{-10}$ sec . . . . .	51
X. Detailed Rates at $1 \times 10^{-5}$ sec . . . . .	52
XI. Comparison of the Eigenstate Rate Equation Solution with the Dual-Based Maxwell-Boltzmann Distribution . . . . .	53

## SECTION I INTRODUCTION

The development of high-temperature devices which will create a high-energy, partially ionized gas (plasma) as a laboratory tool has increased the importance of theoretically predicting the number density distribution of excited states of the plasma components. Without this theoretical grounding, experimental observations will never be removed from a purely phenomenological basis. The many physical processes which generate a specific number density distribution of excited states in a given plasma are strongly coupled so that it is extremely difficult to calculate this population density distribution on anything other than a statistical basis.

Two principal models have been used to describe the population density distribution of a plasma: the local thermodynamic equilibrium (LTE) model and the corona model. Each model uses a different mechanism for the equilibrating process; the LTE model uses collisions between atoms and electrons as the major vehicle for transitions of an atom from one energy state to another, whereas the corona model uses collisional ionization and radiative recombination as the dominant mechanism (Ref. 1). The LTE model is useful only when the electron density is sufficiently high to maintain strong collisional dominance, whereas the corona model applies to the low density situation.

In 1962, Bates, Kingston, and McWhirter (Ref. 2) examined the detailed equations describing the time rate of change of each energy state available to the plasma in terms of the change rate for each individual mechanism. These detailed eigenstate rate equations contain all the physical processes involved in the transient plasma population density distribution and, in the respective limits, reduce to either the LTE or the corona model. Even so, the mathematical description is still quite complicated, and solution is difficult. However, the resultant system of equations does lend itself to simplification for application to many problems of physical interest. In these applications, many of the time derivatives can be set to zero and computation is considerably simplified. This is called the quasi-steady-state approximation and is the problem to which Bates, Kingston, and McWhirter (Ref. 2) addressed themselves in the development of their collisional-radiative recombination (CRR) model. Other investigators (Refs. 3 and 4) used the same approximation in their studies.

The present work, which is an extension of preliminary results reported in 1967 (Ref. 5), is a detailed study of the transient behavior of

a high temperature hydrogen plasma without the quasi-steady-state restriction. Thus, it will be possible to determine if the quasi-steady condition which can be imposed on physical grounds is a natural result of the rate equations or if the imposition of this quasi-steady state is a mathematical condition which is unnatural to the system. By obtaining the fully transient solution to the rate equations, it is also possible to examine in detail the transition to the quasi-steady-state distribution and to determine if there are any radical departures from theory during that portion of the decay. Lastly, if the quasi-steady state is a natural result of the rate equations, the transient solution will indicate the length of time before this condition is established.

Included in the study of the convergence to the quasi-steady state must be the examination of the fundamental consistency of the model. A result of statistical mechanics is that an ensemble of particles in which collision processes are dominant will exhibit a Maxwell-Boltzmann (MB) distribution among the allowed energy states (Ref. 6). Coupled with the fact that many of the collisional rate coefficients in the mathematical model depend for their value on a Maxwellian energy distribution of the exciting particle, then one would expect the transient solution to yield an MB-like distribution among the excited states. Any contradiction would tend to discredit the solution, or the model, or both.

The eigenstate rate equations include all the important physical phenomena governing the population density distribution. By examining detailed terms in the transient solution, it will be possible to study such general properties as equilibration of various specific processes, coupling between several processes, and the subsequent gross properties of the excited state relaxation. These studies will provide valuable insight into the fundamental properties of high excitation temperature gases beyond the specific one studied here.

The existence of a critical level is an important concept in the study of excited state number density distributions in plasma. The critical level, by definition, is the lowest atomic level which exhibits Saha equilibrium with the free electron density (Ref. 2). It has been studied in the past by equating ionization and recombination rates and then establishing that level in which they were equal as the critical level (Refs. 7 and 8).

If the critical level does indeed exist (as one would intuitively expect), then the location should be a natural result of the solution to the full set of rate equations. Further, the transient behavior of the critical level can be studied; e. g., do all eigenstates above the critical level suddenly exhibit the Saha density, or is it truly a transient situation in which the

various levels exhibit the condition at a different time? The solution to the full set of eigenstate rate equations should answer these questions with a minimum of preconceptions imposed on the model.

Specifically, this study will examine two hydrogen plasmas, identical except that one has a metastable atomic level whereas the other does not. (A metastable atomic level is an eigenstate in which the dipole optical selection rules do not allow spontaneous transition to deplete that particular level. In the case of hydrogen, there are no dipole forbidden transitions but the  $2S_{1/2}$  level has a very small probability of an optical transition and will thus be considered as metastable in this discussion.) There has been experimental evidence (Ref. 9) that the presence of a metastable level in some atomic plasmas will significantly affect the observed spectral line intensities. In order to include the metastable level in the calculations, it is necessary to include angular momentum in the quantal description of the plasma and the subsequent mathematical model. It is in the selection rules on the angular momentum that the condition causing the metastability usually arises. To the writers' knowledge, this is the first study of the rate equations which goes into sufficient depth to include the angular momentum. This is not too surprising, however, because of the serious lack of knowledge concerning the angular momentum dependence of the collisional terms. Indeed, only the angular momentum dependence of the spontaneous radiative transition probabilities is known with any degree of confidence. Including the angular momentum dependence would not be justified were it not for the need to study the specific effects of the existence of the metastable level.

At the same time that the effect of the metastable atoms on the spectral intensities was studied (Ref. 9), Brewer and McGregor proposed a simple dual-based MB distribution to describe the excited state population distribution which appeared to be consistent with the experimental results. Since the eigenstate rate equations contain all of the important physical mechanisms indigenous to a thermal plasma, and therefore should yield physically correct results, one of the objectives of this study is to test the validity of the dual-based MB distribution in this application.

In a recent article (Ref. 10), Gordiets, Gudsenko, and Shelepsin also attacked the transient solution of the eigenstate rate equations. Their concern was with the problem in which the excitation temperature experiences a sudden step-function change, and they did not include the angular momentum. Since the work reported herein is concerned with the afterglow problem in which the excitation temperature is constant, no direct comparisons can be made. However, their work shows

essential agreement with that reported in 1967 (Ref. 5) and other unreported work by these authors.

## SECTION II MODEL

### 2.1 THEORETICAL MODEL

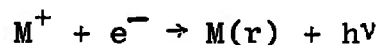
The collisional-radiative recombination model of an ionized gas as developed by Bates, Kingston, and McWhirter (Ref. 2) describes the quasi-steady-state behavior of an optically thin, hydrogenic plasma. In the CRR model, conditions were assumed to have adjusted to the point that the subsequent transient behavior of the plasma is characterized solely by the transient behavior of the ground state and the free electron population density. However, the complete set of differential equations from which the CRR model is developed will describe the transient behavior of the population densities of all states as well as the continuum density, which is the object of the present investigation.

It will be assumed that population changes occur only as a result of radiation or of collisions involving free electrons. The problem is thus restricted to plasmas in which the electron velocity distribution is Maxwellian and the mean electronic velocity is so much greater than the mean velocity of the heavy particles that the latter will be considered motionless (Ref. 11).

Each mechanism causing a change in the population density of a particular eigenstate can be characterized by a rate coefficient. The instantaneous rate by which the level is being populated or depopulated by a given mechanism is the product of the rate coefficient and the number densities of the participants.

Five important mechanisms by which the population density of a particular level can change are considered:

1. Radiative Recombination. In this process, an ion captures a free electron into the  $r$ th electronic state with the emission of a photon:



This reaction will be described by a coefficient,  $\beta(r)$ , so that

$$\frac{dn(r)}{dt} = n^+ n_c \beta(r) \quad (1)$$

is the instantaneous rate of filling of the  $r$ th state caused by radiative recombination. In Eq. (1),  $n(r)$  is the population density of the  $r$ th state,  $n^+$  is the ion density, and  $n_c$  is the electron (continuum) density.

2. Spontaneous Radiative Transitions. For this mechanism, a neutral atom in the  $r$ th quantum state relaxes spontaneously to the  $s$ th quantum state with an attendant emission of radiation:



This reaction is described by the Einstein transition probability,  $A(r, s)$ , so that the instantaneous rate for this process is

$$\frac{dn(s)}{dt} = n(r) A(r, s) \quad (2)$$

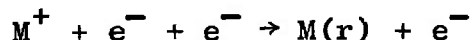
3. Two-body Internal Transition. This is a reaction in which a neutral atom in the  $r$ th state collides with a continuum electron and makes a transition to the  $s$ th state with the necessary energy:



This reaction will be described by  $K(r, s)$  and the rate by

$$\frac{dn(s)}{dt} = n(r) n_c K(r, s) \quad (3)$$

4. Three-body Recombination. For this, a singly ionized atom has an encounter with two continuum electrons. The ion captures one of the continuum electrons into the  $r$ th eigenstate and the excess energy is carried off as kinetic energy of the second electron rather than radiative emission:



The rate constant for this process is  $K(c, r)$ , and the rate is given by

$$\frac{dn(r)}{dt} = n_c n^+ K(c, r) \quad (4)$$

5. Two-body Ionization. This is the inverse of three-body recombination in which a continuum electron collides with and ionizes a neutral atom in the  $r$ th eigenstate:



This reaction is characterized by  $K(r, c)$  and the rate is

$$\frac{dn(r)}{dt} = -n_c n(r) K(r, c) \quad (5)$$

In addition, there are two other mechanisms which may be important in atomic plasmas. These are photon absorption in which a photon emitted by process (1) or (2) above is absorbed before it leaves the plasma, and induced emission in which emission from an excited atom is enhanced by the presence of other radiation of the proper frequency. Neither of these effects is significant in this approximation because of the low densities considered.

The time differential equation for the population density of some state characterized by the principal quantum number  $p$  and angular momentum quantum number  $\ell$  will then be the summation of all these effects, or

$$\begin{aligned} \frac{dn(p, \ell)}{dt} = & -n(p, \ell) n_c K(p, c) - n(p, \ell) n_c \sum_{\substack{q=1 \\ q \neq p}} K(p, q) \\ & - n(p, \ell) \sum_{q < p} \sum_{m=0}^{q-1} A(p, \ell; q, m) \\ & + n_c \frac{2\ell + 1}{p^2} \sum_{\substack{q=1 \\ q \neq p}} \sum_{m=0}^{q-1} n(q, m) K(q, p) \quad (6a) \\ & + \sum_{q=p+1} \sum_{m=0}^{q-1} n(q, m) A(q, m; p, \ell) \\ & + n_c n^+ \frac{2\ell + 1}{p^2} K(c, p) + n_c n^+ \frac{2\ell + 1}{p^2} \beta(p) \end{aligned}$$

In the summation of  $A(p, \ell; q, m)$ , the values are such that the value is zero if the optical selection rule is violated,  $\ell - m \neq \pm 1$ .

In this equation, the first three terms describe the depopulation of the  $(p, \ell)$  quantum state by collisional ionization (Eq. (5)), two-body internal collisional transitions (Eq. (3)), and spontaneous radiative decomposition (Eq. (2)), respectively. The last four terms describe the filling of the  $(p, \ell)$  state via two-body internal collisional transitions (Eq. (3)), spontaneous radiative transitions (Eq. (2)), three-body recombination (Eq. (4)), and radiative recombination (Eq. (1)), respectively. The  $(2\ell + 1)/p^2$  factor arises as a weighting factor for those terms for which the angular momentum dependence is not known.

There will be a similar equation for each eigenstate of the atom, and the instantaneous population density of each state depends on the density of all other levels. In addition, the continuum density,  $n_c$ , enters the equation as a product with other population densities. Thus, there is an infinite, rectangular, coupled, and nonlinear system of equations. However, by considering all of space being filled with this plasma, with no density gradients and no sources or sinks so that the total number of nuclei remains constant and that for hydrogen the continuum and ion densities are identical, then the equation of particle conservation

$$\sum n(p, \ell) + n_c = \text{constant} \quad (6b)$$

added to the rectangular system of equations represented by Eq. (6a) causes the system to become square and, at least in principle, determinate. The solution to this system will give a complete temporal description of the population density of every quantum level available to the atom and the continuum density.

As can be seen, the limit of the applicability of the system of equations (Eq. (6)) to physical problems lies in the ability of the various definitions of the rate coefficients to accurately describe the population density changes due to the various processes. In this simple form, it is obvious that any further physical mechanism which might affect the number density distributions can be taken into account merely by describing the process by an equation similar to Eqs. (1) through (5) and adding the term to Eq. (6a) with the proper algebraic sign.

It should be noted again that the system of equations (Eq. (6)) is descriptive only for those cases in which the sole mechanism for the population density distribution is transitions of the electronic level.

There is no provision within the present scope of the problem for spatial variations in the population densities.

## 2.2 REDUCTION OF THE THEORETICAL MODEL

If the plasmas of interest are confined to those in which the population densities of high atomic levels are considerably less than that of the continuum, the system of equations may be truncated at some finite quantum number with little sacrifice in the accuracy of the model. Thus, in effect, the plasma having an infinite number of allowable states has been replaced by one which has only a finite number of allowable states. This is not quite as artificial as it at first seems because the eigenstate energies get closer and closer together approaching the continuum. With the various levels lying very close together and the excited electrons physically removed in distance from the nucleus, adjustments in the population densities of the upper levels caused by interaction with the continuum take place readily. There is little discernible effect on neighboring levels and virtually no effect on the lowest lying levels caused by these adjustments. Since these higher level population densities are insignificant, numerically, with respect to the continuum and since the magnitude is determined almost solely by interactions with the continuum, they can be neglected. Note that this is, in effect, postulating the existence of the critical level. However, if it is an impossible condition, then the solution to the full system of rate equations should so indicate, regardless of where the system is truncated.

## 2.3 COLLISIONAL-RADIATIVE RECOMBINATION MODEL

A further simplification made by other investigators (Refs. 2, 3, and 4) is the quasi-steady-state approximation in those plasmas in which the population density of the ground state is very much larger than that of all higher states. An equilibrium configuration among these upper states is established almost immediately, and because of this equilibrium, the rate of change of the number densities is very small compared with the rate of change of the ground state. Mathematically this means that, in the system of equations represented by Eq. (6), the derivatives of all states with  $p > 1$  can be set to zero. The rate of growth of the ground state is then numerically the same as the decay of the continuum or electron density.

Thus, the system of equations (Eq. (6)) now becomes one differential equation for the ground state and a system of homogeneous algebraic

equations for the excited states. These algebraic equations are obtained by setting the time derivatives on the left side of Eq. (6a) to zero. The equation for the ground state can be further simplified by writing

$$\frac{dn(1)}{dt} = \alpha n_c^2 - S n(1) n_c \quad (7)$$

where  $\alpha$  and  $S$  are the CRR coefficient and collisional-radiative ionization coefficient, respectively, described by Bates, Kingston, and McWhirter (Ref. 2).

The system of equations can be reduced so that  $\alpha$  and  $S$  can be expressed only as functions of  $n_c$ ,  $T$ , and atomic parameters. The determination of  $\alpha$  and  $S$  was the problem to which Bates, Kingston, and McWhirter addressed themselves.

## 2.4 CRITICAL LEVEL

A simplification even more fundamental than the quasi-steady-state approximation is that of the concept of the critical level (Ref. 2). As defined in Section I, the critical level is the lowest atomic level that exhibits Saha equilibrium with the continuum. If any atomic level,  $p$ , does exhibit Saha equilibrium, then its population density is given by a modified Saha equation (Ref. 12):

$$n(p) = \left( \frac{h^2}{2\pi m_e kT} \right)^{3/2} n_c^2 p^2 \exp(I_p/kT) \quad (8)$$

where  $h$  is Planck's constant,  $k$  is Boltzmann's constant,  $m_e$  is the electronic mass,  $T$  is the excitation temperature, and  $I_p$  is the ionization potential of the  $p$ th state. If in the developing solution of the rate equations some level does exhibit Saha equilibrium, then subsequently its time rate of change can be expressed by the time derivative of Eq. (8). It must be realized at this point that, for this substitution to be valid, the transitions induced by interactions with the free electrons must dominate radiative mechanisms.

The existence and location of this critical level is most important to subsequent calculations. Levels above it will have their population densities given by the comparatively simple relationship (Eq. (8)) which in turn negates the necessity of more involved calculations. If the critical level occurs sufficiently near the ground state as has been indicated

(Refs. 7 and 8), the system of rate equations (Eq. (6)) can be substantially simplified.

## 2.5 DUAL-BASED MAXWELL-BOLTZMANN DISTRIBUTION

If an atom has a metastable atomic level, then an electron in this particular energy level can be removed only by collisional mechanisms. This means that in a large aggregate of such atoms, the metastable level would act as a pseudo ground state and the population density of that level would appear abnormally high. Brewer and McGregor (Ref. 9) proposed a simple model to describe the population densities of those levels above the metastable level which are collision dominated. They proposed that the population densities of these levels were given by the sum of two MB-like distributions. One of these uses the ground-state population of the atom for its base, and the other uses the metastable level population for its base. Or simply,

$$N_n = N_o g_n \exp(-E_n/kT) + N_m \frac{g_n}{g_m} \exp[-(E_n - E_m)/kT] \quad (9)$$

where  $N$  is the population density,  $g$  is the statistical weight, the subscript  $n$  indicates the particular level of interest,  $o$  the ground state, and  $m$  the metastable state. It should be noted that  $N_m$ , rather than being the total number density in the metastable level, will be the excess number density beyond that given by the ground-state-based MB distribution. That is

$$N_m = (N_m)_{\text{total}} - N_o g_m \exp(-E_m/kT) \quad (10)$$

It should also be noted that  $N_o$  in Eqs. (9) and (10) is the actual population density of the ground state and not the total particle number density. The  $N_o$  is related to the total particle density by the partition function in the usual manner.

## SECTION III RATE COEFFICIENTS

Although the rate coefficients described briefly in Section 2.1 are not the objects of this study, they are a critical component of the model. The value of the rate coefficient is related to the probability that a

particular type of transition will occur and that the magnitude will indicate the relative importance of the various mechanisms. In this study, no attempt was made to obtain fundamental information concerning the rate coefficients for the hydrogenic plasmas, but rather the same sources were used as Bates, Kingston, and McWhirter (Ref. 2) to facilitate comparison of results.

### 3.1 EINSTEIN PROBABILITIES, $A(p,q)$

The Einstein spontaneous transition probabilities were evaluated using the radial matrix elements for hydrogen listed by Green, Rush, and Chandler (Ref. 13). For this calculation, the probability of spontaneous transition from the state  $(p, \ell)$  to the state  $(p', \ell')$  is given by

$$A(p, \ell; p' \ell') = \frac{64\pi^4 \nu^3}{3hc^3} \frac{\max(\ell', \ell)}{2\ell + 1} e^2 a_0^2 \langle p' \ell' | r | p \ell \rangle^2 \quad (11)$$

where  $h$  is Planck's constant,  $C$  is the speed of light,  $\nu$  is the frequency of the emitted radiation,  $e$  is the electronic charge, and  $a_0$  is the first Bohr radius. The matrix elements

$$\langle p' \ell' | r | p \ell \rangle = \int_0^\infty R(p', \ell') r R(p, \ell) r dr$$

are listed in their paper for angular momentum values through a principal quantum number of 20. The term  $R(p, \ell)$  above denotes the hydrogen radial wave function.

Since the probabilities are readily available by using Green, Rush, and Chandler (Ref. 13) and Eq. (11) as well as many other sources (Refs. 14 and 15, for example) and because of the large bulk of the data, the values used in this study are not listed. Rather, the reader is referred to any of the above mentioned sources.

### 3.2 RADIATIVE RECOMBINATION, $\beta(p)$

The radiative recombination coefficients,  $\beta(p)$ , for hydrogen were evaluated using a series expansion approximation:

$$\beta(p) = B \left[ 1 - \frac{1}{x} + \frac{2}{x^2} - \frac{6}{x^3} + \frac{24}{x^4} \right]$$

$$B = \frac{64}{3h^3} \alpha^4 a_0^2 \left( \frac{\pi h R}{3kTc} \right)^{1/2}$$

$$x = \frac{157890}{T} \tag{12}$$

where  $\alpha$  is the fine structure constant and R is the Rydberg wave number to the actual values which can be obtained from Seaton (Ref. 16). The values used in this study are presented in Table I (Appendix II).

**3.3 COLLISIONAL RATE COEFFICIENTS, K(p,q), K(p,c), K(c,p)**

The collisional rate coefficients for hydrogen are obtained by integrating the collisional cross sections over the MB energy distribution available for the excitation. This is (Ref. 17)

$$K(p,q) = 8\pi m_e^{-1/2} (2\pi kT)^{-3/2} \int_{E_p - E_q}^{\infty} Q(p,q) \exp(-E/kT) E dE \tag{13}$$

where Q is the cross section for the collision.

The Gryzinski method for determining the cross sections (Ref. 18) appears to be the best available for these determinations and has been used by most investigators. In the most useful form, the expression for collisional excitation is

$$K(p,q) = C \int_1^{\infty} D \exp \left( - \frac{157890(q^2 - p^2)y}{p^2 q^2 T} \right) dy$$

$$D = \frac{[2 - a + y(1 + 4a)](y - 1)^{1/2} (a + 1)^{1/2}}{3a^{1/2} (a + y)^{3/2}}, \quad y \leq a + 1$$

$$D = \frac{[-3a+y(3+4a)] y^{1/2}}{3(a+y)^{3/2}}, \quad y \geq a+1$$

$$C = 8\pi^2 e^4 m_e^{-1/2} (2\pi kT)^{-3/2} \frac{p^2}{q(q^2 - p^2)}$$

$$a = \frac{q^2}{q^2 - p^2}$$

(14)

Gryzinski's expression for the ionization cross section

$$Q = \frac{\pi e^4}{E_1^2} g(x)$$

$$g(x) = \frac{1}{3} \frac{5x-6}{(x+1)^{3/2} \sqrt{x}}, \quad x \geq 2$$

$$g(x) = \frac{4\sqrt{2}}{3x} \left( \frac{x-1}{x+1} \right)^{3/2}, \quad x \leq 2$$

$$x = \frac{E_2}{E_1}$$

where  $E_2$  is the energy of the incident electron and  $E_1$  is the energy of the bound electron, yields for the collisional ionization rate coefficient

$$K(p, c) = \frac{8\pi^2 e^4}{\sqrt{m}} (2\pi kT)^{-3/2} \int_1^{\infty} D \exp\left(-\frac{157890x}{p^2 T}\right) dx$$

$$D = \frac{4\sqrt{2}}{3} \left( \frac{x-1}{x+1} \right)^{3/2}, \quad x \leq 2$$

$$D = \frac{1}{3} \frac{(5x-6)\sqrt{x}}{(x+1)^{3/2}}, \quad x \geq 2$$

(15)

The inverse collision integrals are given by

$$K(q,p) = \frac{p^2}{q^2} \exp \frac{157890(q^2 - p^2)}{p^2 q^2 T} K(p,q), \quad q > p$$

for deexcitation from the qth to pth state, and

$$K(c,p) = h^3 (2\pi mkT)^{-3/2} p^2 \exp \left( \frac{157890}{p^2 T} \right) n_c K(p,c) \quad (16)$$

for recombination from the continuum to the pth state.

The values used in this study were computed in the program and are presented in Tables II and III for  $K(p,c)$  and  $K(c,p)$ , respectively. The values of  $K(p,q)$  are presented in Table IV.

### 3.4 DISCUSSION OF THE RATE COEFFICIENTS

It is apparent, from an examination of the tables of rate coefficients, that their values fluctuate over wide ranges. However, to determine the relative importance of each of the various processes that a rate coefficient characterizes, it is necessary to examine not the coefficients themselves, but the entire term in the rate equations, Eqs. (1) through (5). This requires a more complete quantitative description of the population densities in the plasma. These in turn, depend on solution of the entire set of equations, which is the object of this work. Therefore, a more detailed discussion of the relative importance of the processes as applied to the specific problems being studied here will be deferred to Section V, where the additional data are introduced.

## SECTION IV NUMERICAL ANALYSIS

General analytic methods are not available for nonlinear coupled systems such as those represented by Eq. (6). However, there are a number of numerical methods which can be applied easily with the use of a digital computer.

The particular technique used was chosen because the terms involved in the solution have a direct physical meaning without separate computation as would be the case with less direct methods. That is, most quantities of physical significance appear directly in the calculation rather than occurring implicitly as in other methods. It has the drawback, however, of potentially requiring more computer time to obtain the solution than would be necessary by other means.

#### 4.1 THEORY

By noting that the population density and its derivatives for a given quantum level must be single-valued, finite, and continuous throughout all time, the population density can be written in terms of its time-dependent Taylor's Series:

$$n(p, \ell) = n_0(p, \ell) + \sum_{i=1}^{\infty} \frac{1}{i!} \left. \frac{d^{(i)} n(p, \ell)}{dt^{(i)}} \right|_{t=t_0} (t-t_0)^i$$

This expression is valid provided the series converges, which will be governed by the derivatives as well as the magnitude of  $(t-t_0)$ .

Although any physical process is convergent, the problem being dealt with is the mathematical representation of a physical process, and this representation may or may not be convergent. However, if the function  $n(p, \ell)$  is well behaved, the Taylor's Series representation will be convergent. The functional form of  $n(p, \ell)$  is not known, only a representation of derivatives. However, examining succeeding time derivatives of the system represented by Eq. (6) shows that the  $i$ th derivative will be dependent only on products and sums of lower derivatives of the system, that no functional singularity is apparent, and that the function should be well behaved and thus the series should be convergent.

In the above discussion, referring to the system of equations, Eq. (6), it was assumed that an infinite number of terms can be carried in the series. Realistically, this is not the case, but rather a finite series is used, such as

$$n(p, \ell) = n_0(p, \ell) + \sum_{i=1}^I \frac{1}{i!} \left. \frac{d^{(i)} n(p, \ell)}{dt^{(i)}} \right|_{t=t_0} (t-t_0)^i \quad (17)$$

where now  $I$  must be chosen so that errors introduced by neglecting those terms for  $i > I$  can be considered as insignificant in the calculation. Or, conversely, some  $I$  can be chosen, and in turn, a  $t$  can be chosen so that the truncated terms are negligible. Thus by choosing some  $t_{\max}$  so that the terms for  $i > I$  are insignificant compared with those terms for  $i \leq I$ , then the finite series can be used to give a sufficiently accurate solution for  $n(p, \ell)$  for any  $t \leq t_{\max}$ .

Hence, it is possible to find the solution for  $n(p, \ell)$  in time by using the system of equations, Eq. (6), to find all higher derivatives at  $t = 0$ , to examine these derivatives to determine what  $\Delta t = t - t_0$  must be to ensure convergence, and to evaluate the series to find  $n(p, \ell)$  for all  $p$  and  $\ell$  considered. Then it is possible to return to the system, to recompute the derivatives for this new distribution, to find a new  $\Delta t$ , and to repeat the calculations until all desired information is acquired. Thus, the actual transient problem is considered as a series of initial value problems; the solution over one time interval provides the initial value for the next time interval.

## 4.2 APPLICATION

From the discussion in the preceding paragraph, the larger the value of  $I$ , the larger the factor  $(t-t_0)$  may be. However, there will naturally be an upper limit because of machine limitations, both from the aspect of size as well as the sheer magnitude of the numbers involved. Similarly, there will be a limit to the number of quantum states which can be considered because of the size of the machine utilized in the solution.

The number of terms retained in the series will have a direct influence on the real plasma time. Therefore, the program to solve the system of equations, Eq. (6), was written in order to use an arbitrary number of derivatives to a limit of  $I = 10$ . The actual number of terms kept for the evaluation via Eq. (17) was then determined by the magnitude of the derivatives so that no attempt was made to use a derivative which would cause machine overflow. By having the number of terms in the series, Eq. (17), thus determined, the factor  $(t-t_0)$  was chosen to yield convergence. It should be noted that, for the particular problem studied here, the condition  $I = 10$  was never realized, but rather the magnitude of succeeding derivatives was such that the series truncated at smaller values of  $I$ .

As discussed in Section 2.2, the system of equations, Eq. (6), can be truncated above some quantum level without significantly affecting the

solution. One of the objectives of this study was to examine any rapid adjustments in the number density distributions between the uppermost atomic levels. This would indicate considering a large maximum quantum number. However, the size of the computer used dictated that a principal quantum number of 10 would be the maximum number which could be considered. By including the angular momentum, the system of equations, Eq. (6), becomes a 56 by 56 system.

This should not be a serious limitation on the principal quantum number for illustration of the upper level adjustments however. Drawin (Ref. 3), in his study of the quasi-steady-state solution, showed that truncation of the system at a quantum level of 10 should cause no significant numerical error. If the critical level established itself at the predicted level (Refs. 7 and 8), the maximum quantum number 10 will include enough states above the critical level for examination of detailed processes.

#### 4.3 EXTRAPOLATIONS

Since the CRR model depends on the first time derivatives of the excited states being zero with respect to that of the ground state, it is expected that the transient solution will converge to this CRR model as the upper states come into equilibrium with the continuum.

As this equilibrium condition is approached, the actual solution will become quite flat in time, and it should be possible to approximate the solution by some curve fit over comparatively long periods of time. Such an approximation will considerably speed computation of results. Consequently, this device was used in the actual solution of the problem. By using values of the populations and derivatives from the system solution to determine the slope and intercept, the population densities were extrapolated by straight lines. These extrapolations were never allowed to extend forward in time far enough to change any population density by more than 5 percent, however. After each extrapolation, the full system was used so that the perturbations introduced by the extrapolation could damp out.

Another technique utilized to speed computations was the use of the Saha equation (Eq. (8)) to compute the time derivatives of those states which exhibited Saha equilibrium. This, of course, subsequently ensured that those levels would satisfy Saha equilibrium, but periodically the full model was used as a check. Invariably, the Saha equilibrium density for that level was found to satisfy the full system within a small error.

#### 4.4 REPORTING OF DATA

The discussion to this point has included all angular momentum values which the hydrogen atom may have. The problem was solved including these angular momentum distinctions, even through expressions for the angular momentum dependence of the collisional rate coefficients are not available. The only place in this study that this dependence has anything other than a purely statistical effect is in the spontaneous radiative transition probabilities,  $A(p, q)$ . Further, because of the conditions of the plasmas studied, this distinction has no quantitative effect except on the two lowest quantum levels, and their subsequent effect on the plasma distribution as a whole. Consequently, the data which are reported in the following section are shown as though there were no angular momentum distinction except for the aforementioned eigenstates.

### SECTION V RESULTS OF COMPUTATIONS

The numerical solution to the system of eigenstate rate equations was examined to satisfy several objectives:

1. To determine if the fully transient solution will yield a population density distribution which is MB for strongly collision dominated levels. If this is not the case, the mathematical model must be revised before meaningful physical interpretations can be applied to the results. Once one is satisfied with the fundamental consistency of the model, the solutions may be examined to provide physical insight into the mechanisms by which equilibration, decay, and growth of the various excited state population densities occur.
2. To examine the existence and location of the critical level.
3. To make a quantitative examination of the solution to the eigenstate rate equations for the metastable and nonmetastable case. Also, the relative importance of the various terms in the rate equations themselves can be examined.
4. To compare the time development of the population density distribution of the metastable atomic plasma with the time development of the atomic plasma with no metastability. The subsequent effects of the metastable level on the radiation from a plasma and the lifetime of the plasma will be examined.

5. To examine the ability of the relatively simple dual-based MB distribution to reproduce the excited state population density distribution.
6. To study the relaxation of the solution to the quasi-steady state and subsequent CRR model.

## 5.1 FUNDAMENTAL CONSISTENCY

Three cases (A, B, and C) were used in the calculations, all at an electron temperature of 10,000°K and a total population density of  $2.6 \times 10^{16} \text{ cm}^{-3}$  (right-hand side of Eq. (6b)) at a pressure of 0.001 atm. The continuum density for each case was chosen to be that which would be in Saha equilibrium with the ground state at that temperature. In cases A and B, the distribution among the upper states was chosen such that the population density of each state was one-half of that which would be given by an MB distribution. In case C, the distribution was fully MB. The distinction between cases A and B is the value of the spontaneous transition probability for the quasi-metastable (2, 0) eigenstate. Case A, which is the metastable case, used a transition probability of 0, whereas case B used a fictitious transition probability of  $6 \times 10^8 \text{ sec}^{-1}$  for this level, thus effectively removing the metastability. Case C was similar to case A in this respect with a metastable level at (2, 0).

The differences in the initial distributions were chosen in order to facilitate checking the fundamental consistency of the solution. For the electron temperature and continuum density chosen, the plasma should be collision dominated. This may be illustrated by the collision frequency from the classical mean free path for an electron in hydrogen gas. Cobine's expressions (Ref. 11) show that, for the conditions of this investigation, the electronic mean free path will be on the order of 0.5 cm with a resultant collision frequency of  $1 \times 10^{23} \text{ encounters sec}^{-1} \text{ cm}^{-3}$ . This is to be compared with radiation terms which will be on the order  $1 \times 10^{14} \text{ transitions sec}^{-1} \text{ cm}^{-3}$ . Thus, case C, which started as an MB distribution, should retain its MB-like character, whereas cases A and B, which were underpopulated with respect to the true MB distribution should rise in number density until they become like case C. Also, cases A and B should retain very similar number densities at least until times on the order of  $10^{-8} \text{ sec}$ , at which time radiative transitions begin to have an appreciable effect.

Figure 1 (Appendix I) illustrates qualitatively the time development of the three cases for one of the eigenlevels above the metastable level.

This behavior was fairly typical of all upper levels. There is no scale in Fig. 1 other than the relative positions of the three curves. Important times are marked on that scale and are correct relative to the character of the three curves. The important thing to note is that case A and case C develop to the same values of population densities for quite different initial distributions, whereas case B has started to depart from these even though it had the same initial distribution as case A and retained, for all practical purposes, the same distribution as case A for small times. Case C exhibited an MB character to its distribution throughout its decay. This evidence, the convergence of the three cases for small times and the retention of the MB characteristics by case C, suffices to establish fundamental consistency of the mathematical model since, for ensembles which are collision dominated, statistical mechanics shows that the distribution should be MB (Ref. 6).

Since cases A and C evolved to very nearly the same values for all densities and parameters while A and B differed much more significantly, the case C computation was terminated after a real plasma time of about  $1 \times 10^{-7}$  sec. It should be noted that the relaxation time for A to become like C was about  $10^{-10}$  sec. The similarity between them suggests strongly that the plasma decays like an MB distribution and that a perturbation that causes the plasma to be initially in a nonequilibrium configuration will damp out and the plasma will come to the equilibrium configuration very rapidly if the perturbation is not maintained. Further, it indicates that, if there should happen to be a perturbational error somewhere in the calculations, the system would return to the true solution path in a plasma time on the order of  $10^{-10}$  sec, which was adjudged to be insignificant physically.

## 5.2 CRITICAL LEVEL

The critical level should make itself evident as the decay progresses. Case C, which was originally required to exhibit Saha equilibrium, retained that characteristic for the eigenstates with  $p \geq 4$  throughout the extent of the computations. Because of radiative effects, the levels below  $p = 4$  departed from the Saha density after times on the order of  $10^{-9}$  sec.

The upper levels of cases A and B, which were not initially Saha in magnitude, approached this value monotonically, and once reached, the level decayed with the continuum, maintaining the population density in Saha equilibrium throughout the calculation.

In the time development of the population densities, the existence of Saha equilibrium occurred in the uppermost level first, and then the highest level at which this occurred moved downward as time increased. Table V shows the time at which Saha equilibrium occurred for the various levels for case A. Case B exhibited approximately the same behavior except that quantum level 4 reached Saha equilibrium at about  $1.5 \times 10^{-7}$  sec. To the extent of the present computations, the quantum level 3 has not exhibited Saha equilibrium for either case.

It is interesting to note that the upper levels 6 through 10 showed Saha equilibrium almost simultaneously, and the distinction in the times at which this occurs for these levels is probably mathematical rather than physical. However, the lag between these levels and level 5 may be physically significant, and certainly the further three orders of magnitude before quantum level 4 exhibits the equilibrium is physically significant.

The results indicated in Table V can be compared with the calculations of Hinnov and Hirschberg (Ref. 8), who show that for electronic energies greater than 0.25 eV (approximately 2500°K), the quantum level 4 would be the critical level.

From the preceding discussion, it is now apparent that the critical level concept, which is vital to simplification of the computations, is indeed valid and that the location is at the level predicted by Hinnov and Hirschberg (Refs. 7 and 8). However, care must be exercised when using this concept in other calculations and laboratory experiments, for if a nonequilibrium situation exists at the beginning of the experiment, then it requires a physically significant time for the final critical level to establish itself. The transient behavior of the critical level is about what would be expected. The upper levels approach equilibrium much faster than the lower levels.

### 5.3 NUMBER DENSITY DISTRIBUTION AND RATES

As a quantitative illustration of the number density distributions and the rates involved in the computation, Tables VI and VII show the initial conditions for the two cases A and B along with the density distribution at a plasma time of  $1 \times 10^{-5}$  sec when the calculations were terminated. The fourth column in each table shows the rate with which each quantum level was changing at the time the calculations were terminated.

The effect of the metastable level is quite evident in these tables. Case A shows a distinct inversion of the population densities of the (2, 0) and (2, 1) levels at a real plasma time of  $1 \times 10^{-5}$  sec. Furthermore, from an examination of the decay rates in column 4 of Table VI, it appears that the inversion will tend to intensify as time progresses. The subsequent effect on the continuum density and excited state population densities is also apparent by the elevated values for case A compared with case B. Note also that the rates of decay, although quite similar, show a tendency for case B to depopulate the upper levels at a slightly faster rate than case A, thus widening the difference in the population densities of the two cases. This is even more noticeable by comparing the continuum density values and rates. Here it is quite obvious that the plasma with the metastable atomic level is relaxing noticeable slower than the nonmetastable atomic level.

More informative of the detailed processes involved is the examination of the contribution of each individual mechanism involved in the decay as described (Eqs. (1) through (5)). For this purpose, Tables VIII, IX, and X show time rates of change for each quantum level for each of the two cases and for the various physical processes considered. Columns T1 through T7 may be compared directly with the seven separate terms in Eq. (6a). By using the nomenclature of Tables VIII, IX, and X, Eq. (6a) would be written:

$$\frac{dn}{dt} = -T1 - T2 - T3 + T4 + T5 + T6 + T7$$

for each (p,  $\ell$ ).

Table VIII is early in the computation when the upper levels are in a nonequilibrium configuration. Table IX gives values when the Saha equilibrium configuration is nearly established among the upper levels, and Table X allows comparison at the time the calculations were terminated. The rates for the two cases were nearly identical at the times of Tables VIII and IX so there is only one entry for each element in the array.

From quantum level 10, for example, in Table VIII, it is obvious that the term presenting the change in the population density via a collision between a neutral atom and a continuum electron, resulting in a change of energy level of the bound electron, is by far the largest of the effects. But, since there is both a populating effect and a depopulating effect and since the initial distribution approximated an equilibrium distribution for this effect (Maxwell-Boltzmann), these two effects

are in near equilibrium ( $T_2 \approx T_4$ ). However, the terms representing change rates in population due to three-body effects are obviously not in equilibrium, with the continuum contributing to the level at roughly twice the rate that the atoms within this level are being ionized ( $T_6 \approx 2 T_1$ ). The other effects are small enough to be unimportant comparatively. Conversely, from Table VIII, level 2, it can be seen that radiation effects ( $T_3$ ) are quite competitive, or even dominate the decay.

Now, an examination of quantum level 10 in Table IX shows that the internal population density changes are still in near equilibrium but that now the three-body terms are also in near equilibrium. In fact, by examining the combination of these effects, it can be seen that the collisional terms are even nearer equilibrium. However, the slight unbalance of the collisional terms still largely dominates the radiative effects.

An examination of Table X, which compares the two cases at the time the calculations were terminated, shows that the four major collision effects are in very near equilibrium and, further, that they are in equilibrium to the extent that the unbalanced contribution to the depopulation of this state is due to spontaneous radiative transitions ( $T_3$ ). The net effect of the collision terms is the population of the upper quantum levels through three-body interactions.

An examination of Tables VIII, IX, and X illustrates the relative importance of various mechanisms in the plasma decay. It is obvious that two-body interactions between the continuum and neutral atoms are the dominant process for population or depopulation of all but the ground state and that three-body interactions run a very close second. But, the collision terms appear to have to dominate the radiative terms by a least three orders of magnitude before a particular level will exhibit equilibrium with the continuum. This is evidenced by the fact that quantum level 4 is in Saha equilibrium, whereas quantum level 3 is not (Tables VI and VII). It should be noted also that, for the number densities used here, radiative recombination is singularly unimportant, being dominated by other processes by several orders of magnitude at all times.

#### 5.4 TIME COMPARISON OF METASTABLE AND NONMETASTABLE CASES

In this section is presented the time development of case A (metastable) and case B (nonmetastable) for comparison of the population density distributions. It should be repeated that, for these comparisons, the initial conditions for the two cases are identical in every way except that case B had a fictitious transition probability of  $6 \times 10^8$

$\text{sec}^{-1}$  for the (2,0) eigenstate while the actual probability is very small, zero in this case. All other atomic parameters are identical, and thus the two cases are consistent for the comparison. Any deviations in the subsequent solution will be solely due to the effect of the developing difference in the metastable level on the rest of the distribution.

Figures 2 through 4 show the time development of quantum levels 3, 5, and 10 for the two cases over the period of time from  $1 \times 10^{-6}$  to  $1 \times 10^{-5}$  sec. Figure 5 illustrates the continuum density over the same time range. In these figures, the coordinate system is Cartesian, with time being the abscissa and population density the ordinate. As is obvious from the figures, the population densities for case A, the metastable case, remain significantly higher than for case B, and the difference between the two is diverging as time progresses. The two cases exhibit a difference in the number densities at a much earlier time than is shown in the figures, but there is no difference in the character of the curves.

The particular quantum levels shown are indicative of all levels except, as would be expected, the ground state and the metastable state. The ground state, for both cases, has steadily populated although at different rates as can be seen in Tables VI and VII. The metastable (2,0) state is shown in Fig. 6. Because of the large ranges of time and number densities involved, Fig. 6 is not drawn to scale, and the comparison is largely qualitative with important quantitative features marked. The particular emphasis here is the physical effect of the metastable (2,0) level on the excited state population density distribution.

An examination of these curves (Figs. 2 through 5) shows that there is a slight flattening with increasing time and that there generally appears to a parabolic character to the curves. This parabolic character was retained when the data were plotted on semilogarithmic scales although the curves were somewhat linearized. Subsequently, the data were least-squares curve fitted in the semilog plane to an equation of the type

$$\ln n = a_1 + a_2 t^{1/4} + a_3 t^{1/2} \quad (18)$$

This equation was used to perform extrapolations for increasing time. Because of the highly qualitative form of the analysis of the existing curve and because of the errors inherent in extrapolation, extreme care must be exercised in how far the extrapolation will be valid.

For these extrapolations, since it is known that the upper levels exhibit Saha equilibrium with the continuum, each extrapolated level density along the extrapolated continuum density was compared with the corresponding Saha factor

$$\frac{n_p}{n_c} = \left( \frac{h^2}{2\pi m_e kT} \right)^{3/2} p^2 \exp(I_p/kT) \quad (19)$$

When there was more than a 15-percent deviation between the extrapolated values and the right side of Eq. (19), the extrapolation was terminated.

Figure 7 shows the time development of quantum level 5 on a log-log graph from a time of  $1 \times 10^{-8}$  to  $1 \times 10^{-4}$  sec. The extrapolation described above was used in the region above  $1 \times 10^{-5}$  sec. This behavior was typical for all the upper quantum levels. As can be seen, the two population densities are, for all practical purposes, the same until about  $5 \times 10^{-7}$  sec when they begin to diverge. By a time of  $1 \times 10^{-5}$  sec, the two differ by roughly 10 percent, and the divergence is accelerating. One of the interesting aspects of this is that the radiation from a gas with a metastable atomic level would be noticeably more intense than radiation from a gas which did not have this metastable atomic level.

Further, an examination of the decay rates in Tables VI and VII shows that the continuum is decaying faster in the case where the metastable level is absent so that the upper levels, which remain in Saha equilibrium with the continuum, are also decaying at a faster rate. Thus, the plasma with a metastable level would have a much longer lifetime than the plasma which does not have this metastable level. Although lifetime calculations are not attempted here, it has been shown experimentally (Ref. 19) that radiation from an argon plasma (argon has a metastable level) can be substantially quenched by mixing into the plasma gases which will accept the metastable energy in collisional processes with the metastable atom. Consequently, when the population density of the metastable atom is depleted, the population density of the upper excited states is also depleted.

Figure 8 illustrates in a Boltzmann plot the time development of the population density distribution for case A. Both cases exhibited the same character on a plot of this kind. Each line is for a selected time as marked. Energy is in electron volts, and the corresponding

quantum number is marked for reference. It is obvious from this that the decay is MB in character and at a constant temperature. This figure graphically illustrates that quantum level 4 is the critical level because all states above it fit the MB distribution with some unknown base, whereas those levels below quantum level 4 do not show the Boltzmann distribution.

In summary, the data presented here have shown quantitatively that, for similar plasma conditions, the metastable atomic level will elevate the population density distribution compared with that in a nonmetastable plasma. Hence, the lifetime of the afterglow is appreciably increased.

### 5.5 DUAL-BASED MAXWELL-BOLTZMANN DISTRIBUTION

As just described, the levels above the critical level decay as an MB distribution, but with an undefined base. Brewer and McGregor (Ref. 9) presented a simple model, described in Section 2.5, to explain radiation from gases containing a metastable atomic level. Subsequent to the termination of solution in the rate equations, the data concerning the first two atomic levels were used to compute two MB distributions, each at 10,000°K. Table XI shows the results of these computations. Column 2 gives the results of the solutions to the rate equations; column 4 gives the results of computing another MB distribution using the excess of the (2, 0) state in the rate equation solution as the ground state population density for the computation. Column 5 represents the sum of columns 3 and 4, which is to be compared with column 2, and column 6 gives the comparison. As can be seen, the agreement between the rate equation solution and the other model is quite good, particularly for those levels which are strongly collision dominated.

The large deviations for the (2, 1) state in columns 5 and 6 are easily explained. This level is not collision dominated, and radiative effects are very competitive with the collision effects. The ability of the MB distribution to predict excited state population densities depends on purely collisional mechanisms for energy transferral. Therefore, any level which is not strongly collision dominated would be expected to deviate from this distribution.

Figure 9 shows graphically a comparison between the rate equation solution and the dual-based MB model. Because of the various computational approximations used to speed the rate equation solution, Table XI and Fig. 9 show more disagreement than was actually present. The approximations used in the rate equations solution would cause perturbational errors in the distribution which would always damp out when the

full system of rate equations was used. Inevitably, when the full system of equations was used, this solution and the dual-based MB would converge. Case B, the nonmetastable case, was also examined in light of this model although there is no basis for comparison and the results were nonsensical.

## 5.6 CONVERGENCE TO THE CRR MODEL

Bates, Kingston, and McWhirter (Ref. 2) reduced the full system of rate equations in order to compute the collisional-radiative recombination and collisional-radiative ionization coefficients ( $\alpha$  and  $S$  of Eq. (7), respectively). The method used for the reduction was to set the time rates of excited state population densities to zero. Thus the rate of growth of the ground state was numerically the same as the decay of the continuum. These coefficients can be computed directly from the transient solution. If Eq. (7) is considered,

$$\frac{dn(1,0)}{dt} = \alpha n_c^2 - S n(1,0) n_c$$

with  $\alpha$  and  $S$  time independent on differentiation with respect to time, Eq. (10) becomes

$$\frac{d^2n(1,0)}{dt^2} = 2 \alpha n_c \dot{n}_c - S [n(1,0) \dot{n}_c + \dot{n}(1,0) n_c]$$

where the dot denotes time differentiation. The transient solution to the rate equations can now be used to generate a simultaneous set which can be solved for  $\alpha$  and  $S$ . The conditions required by the Bates, Kingston, and McWhirter solution for  $\alpha$  and  $S$  were never reached during the calculations because of the various approximations to speed computation. However, during the course of the solution, an artificial condition approximating that of Bates, Kingston, and McWhirter was generated, and the  $\alpha$  and  $S$  determined from this agreed well within the accuracy of the data reported by Bates, Kingston, and McWhirter in their 1962 paper (Ref. 2).

Because the quasi-steady state was never allowed to develop to a sufficient degree for detailed comparison, it is impossible to study this aspect of the rate equation solution in as much depth as would be desired. However, some inference can be drawn from the results. When allowed to progress normally, the first derivatives of the excited state population density tended monotonically toward zero. Even when there were

perturbations in the distribution which could have allowed an instability to develop, this tendency toward zero was retained. This implies that the quasi-steady state will be a natural result of the solution to the set of eigenstate rate equations.

It is impossible to assign a definite time when the derivatives become small enough for the quasi-steady state to be approximated. However, in case C, the true MB distribution, this quasi-steady state had not been established after  $5 \times 10^{-9}$  sec when the Saha relation was used to reduce the system of equations. Indications are that times in excess of  $1 \times 10^{-8}$  sec would be required for this condition to be established.

## SECTION VI CONCLUDING REMARKS

The purpose of this study has been to examine the transient behavior of a theoretical hydrogen plasma using the collisional-radiative recombination model and to learn from the behavior of this plasma some general characteristics of a decaying plasma applicable to other gases. In particular, a comparison of the transient behavior of two similar plasmas, different only in the Einstein radiative transition probability of the (2, 0) atomic level, was made. The results of this study are summarized as follows:

1. The rate equations offer a solution which shows MB-like decay if the collisional terms largely dominate the radiative as is required from statistical mechanics.
2. The critical level does indeed exist and at the level predicted by Hinnov and Hirschberg's analysis (Refs. 7 and 8).
3. Saha equilibrium is established among the upper levels at physically insignificant time ( $\sim 10^{-10}$  sec), but the above-mentioned critical level is not established until a physically significant time ( $\sim 10^{-7}$  sec).
4. The presence of a metastable level in a decaying plasma definitely elevates the population density of the states above it, causing, in effect, the plasma to be longer lived.
5. The population density of the upper levels can be predicted easily, and to a high degree of accuracy, by the dual-based MB distribution (Ref. 9).

6. Solution of the rate equations does indeed reduce to the simple model proposed by Bates, Kingston, and McWhirter (Ref. 2), but it is difficult to place any definite criteria on the application of the model from the present solution. Indications are that the quasi-steady state will not be established until a plasma time has elapsed which is significant compared with measurement time.
7. Any perturbations in the plasma that would cause a slight non-equilibrium configuration will damp out in a time that is small compared with typical measurement times at the temperature of this solution.

The transient solution to the full set of Eq. (6) has quantitatively verified many techniques and substitutions which can be used to simplify the solution. These should be utilized in any future study to facilitate the solution. Although the system solved here has been quite large, the use of, in particular, the Saha equation will reduce the system to a much more manageable one, leaving indeterminate only those levels below the critical level for those times of physical significance.

A study of the transient solution to the rate equations offers a multitude of possibilities for further worthwhile investigations. First, although the present study establishes the validity of the model on theoretical grounds, the model and its solution needs to be further tested experimentally to establish its applicability. The present system of equations, Eq. (6), has been developed only for hydrogenic gases; a corresponding model for some of the rare gases such as helium or argon would greatly illuminate the behavior of decaying plasmas. It would be quite easy also to include the effect of absorption of emitted radiation which is always a possibility when considering a physical plasma.

Although the study here was an afterglow problem (constant excitation temperature), the model provides the means to investigate the problem in which the excitation temperature is not constant but varies in some manner. Also, the spatial terms to describe diffusion and three-dimensional flowing gases with attendant coupling to the temperature and total density could, in principle, be included. These additions would be necessary for direct comparisons with most laboratory experiments.

The model is most useful in providing a means whereby the physical effects of the various rate parameters inherent in the formulation can be studied. Hence, the understanding of plasmas can be greatly benefitted by numerical studies of the various conditions which can be generated.

## REFERENCES

1. McWhirter, R. W. P. "Spectral Intensities." Plasma Diagnostic Techniques, R. H. Huddleston and S. L. Leonard, editors. Academic Press, New York, 1965, pp. 201 to 264.
2. Bates, D. R., Kingston, A. E., and McWhirter, R. W. P. "Recombination between Electrons and Atomic Ions I. Optically Thin Plasmas." Proc. Roy. Soc., A267 (London), 1962, p. 297.
3. Drawin, V. H. W. "Über die Abhängigkeit der Besetzungsdichten der Wasserstoffniveaus von der Nichtthermischen Plasmen." Analen der Physik, Vol. 14, No. 7, 1964.
4. McWhirter, R. W. P. and Hearn, A. G. "A Calculation of the Instantaneous Population Densities of the Excited Levels of Hydrogen-like Ions in a Plasma." Proceedings of the Physical Society, Vol. 82, 1963, p. 641.
5. Limbaugh, C. C., Carstens, J. C., McGregor, W. K., and Mason, A. A. "A Numerical Solution to the Collisional Radiative Model." Paper FA-7 presented at Southeastern Section of the American Physical Society, Clemson University, Clemson, South Carolina, November 1967.
6. Rushbrooke, G. S. Introduction to Statistical Mechanics. Oxford University Press, London, 1964.
7. Hinnov, E. and Hirschberg, J. G. "Spectroscopic Measurements of Helium Afterglow." Proceedings of the Fifth International Conference on Ionization Phenomena in Gases, Munich, Germany, 1961.
8. Hinnov, E. and Hirschberg, J. G. "Electron-Ion Recombination in a Dense Plasma." Phys. Rev., Vol. 125, No. 3, 1962, pp. 795 to 801.
9. Brewer, L. E. and McGregor, W. K. "The Influence of Metastable Atoms on the Population of Excited States in a Thermal Plasma." Proceedings of the Sixth International Conference on Ionization Phenomena in Gases, Paris, France, 1963.
10. Gordiets, B. F., Gudsenko, L. I., and Shelepsin, L. A. "Relaxations of the Occupied Levels of Hydrogen in a Highly Excited Plasma, with Consideration of the Reabsorption of Radiation." Journal of Quantitative Spectroscopic Radiative Transfer. Vol. 8, 1968.

11. Cobine, J. D. Gaseous Conductors. Dover Publications, New York, 1958.
12. Cambel, A. B., Duclos, D. P., and Anderson, T. P. Real Gases. Academic Press, New York, 1963.
13. Green, L. C., Rush, P. P., and Chandler, C. D. "Oscillator Strengths and Matrix Elements for the Electric Dipole Moment for Hydrogen." Astrophysical Journal, Vol. 125, No. 3, 1957, p. 835.
14. Moore, C. E. Atomic Energy Levels. Vol. I. National Bureau of Standards, United States Department of Commerce. Government Printing Office, Washington, 1949.
15. Wiese, W. L., Smith, M. W., and Glennon, B. M. Atomic Transition Probabilities. Vol. I. National Bureau of Standards, United States Department of Commerce. Government Printing Office, Washington, 1966.
16. Seaton, M. F. "Radiative Recombination of Hydrogenic Ions." Royal Astronomical Society Monthly Notices. Vol. 119, No. 2, 1959.
17. Kingston, A. E. "Excitation and Ionization of Hydrogen Atoms by Electron Impact." Physical Review. Vol. 135, No. 6A, 1964, p. A1529.
18. Gryzinski, M. "Classical Theory of Electronic and Ionic Inelastic Collisions." Physical Review. Vol. 115, No. 2, 1959, p. 374.
19. McGregor, W. K. and Brewer, L. E. "The Radiative Decay of Metastable Argon Atoms in a Low-Density Argon Plasma Stream." AEDC-TDR-63-5 (AD294543), January 1963.

**APPENDIXES**  
**I. ILLUSTRATIONS**  
**II. TABLES**

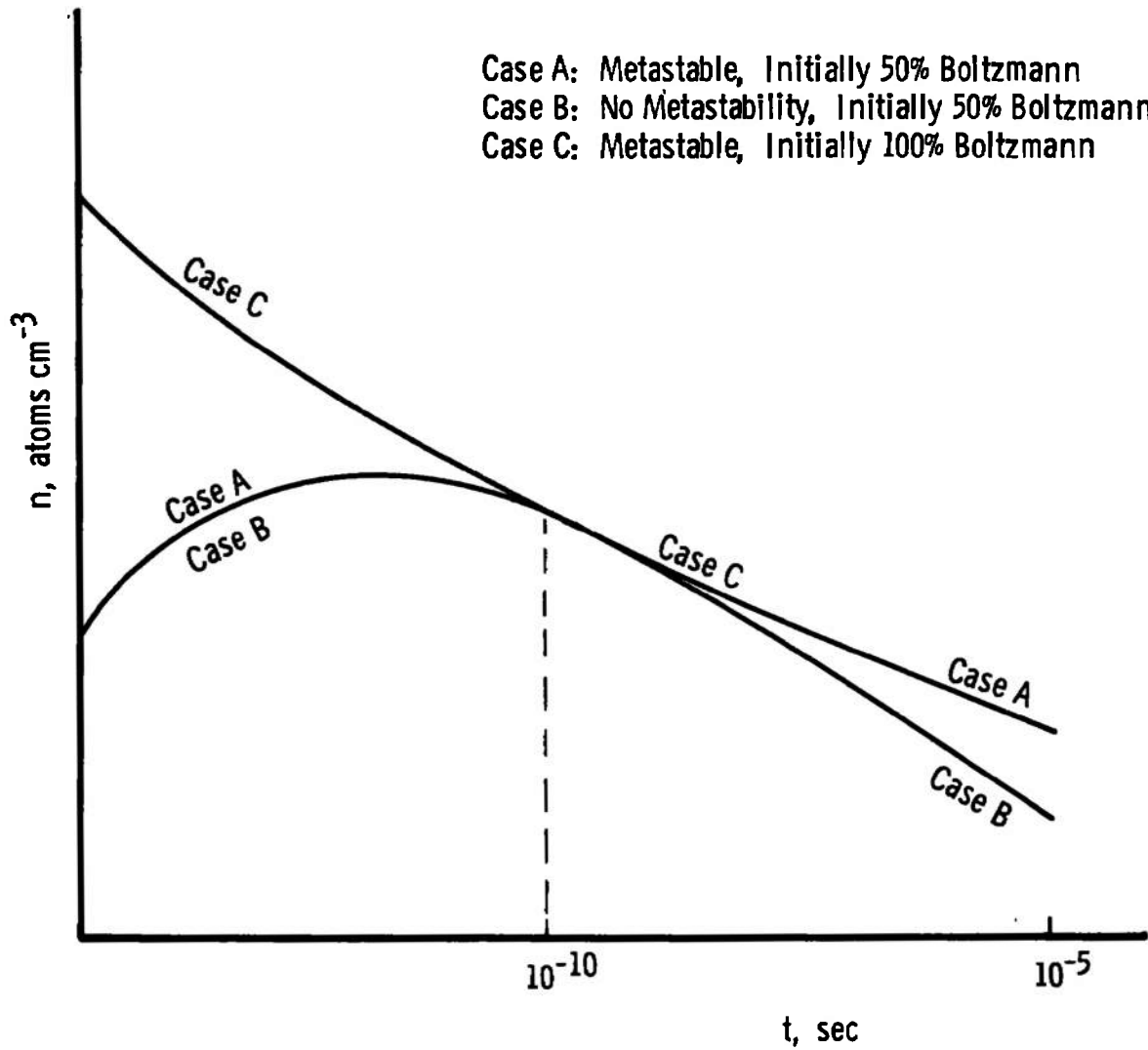


Fig. 1 Time Development of the Test Cases

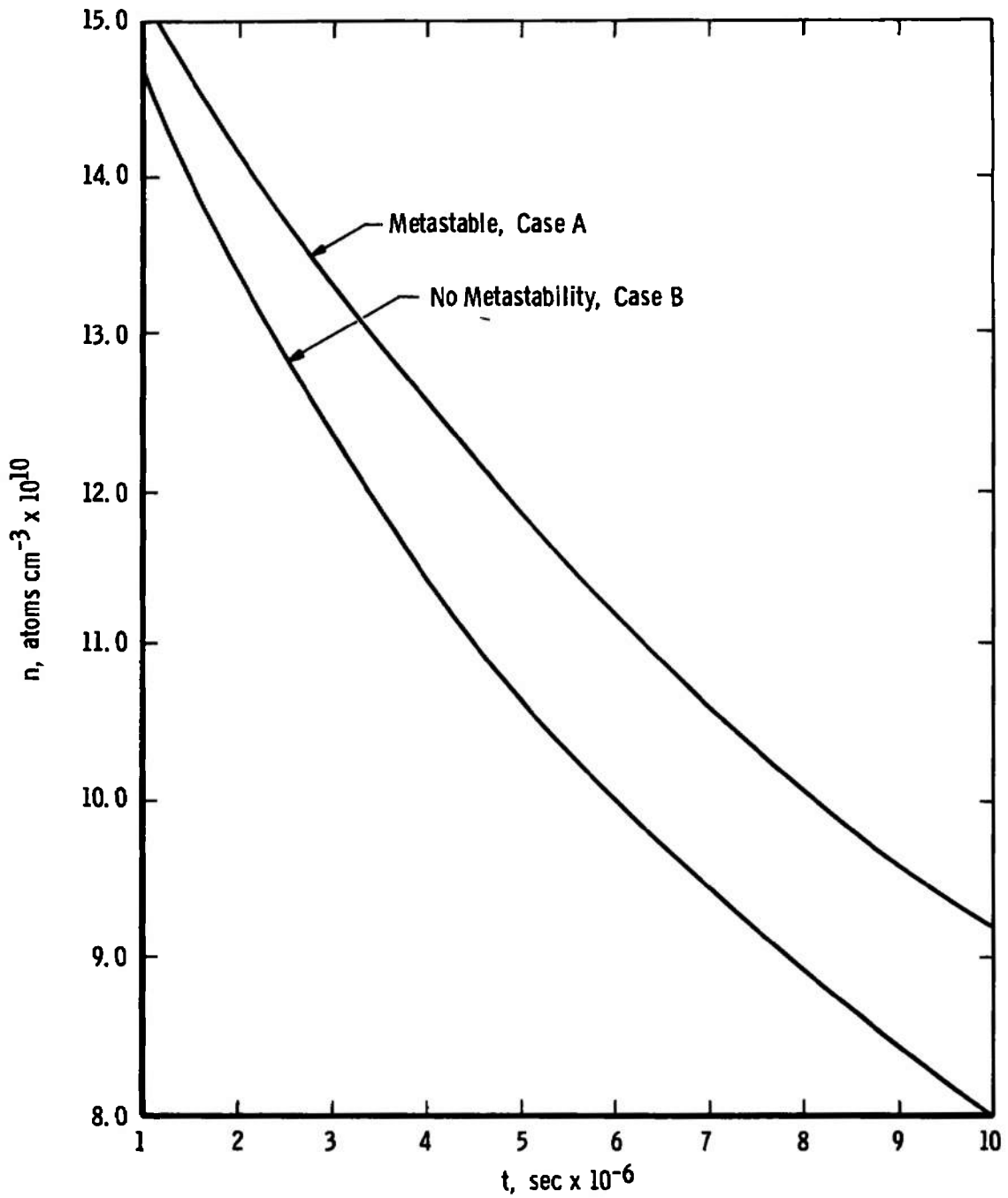


Fig. 2 Comparison of Time Developments of Quantum Level 3

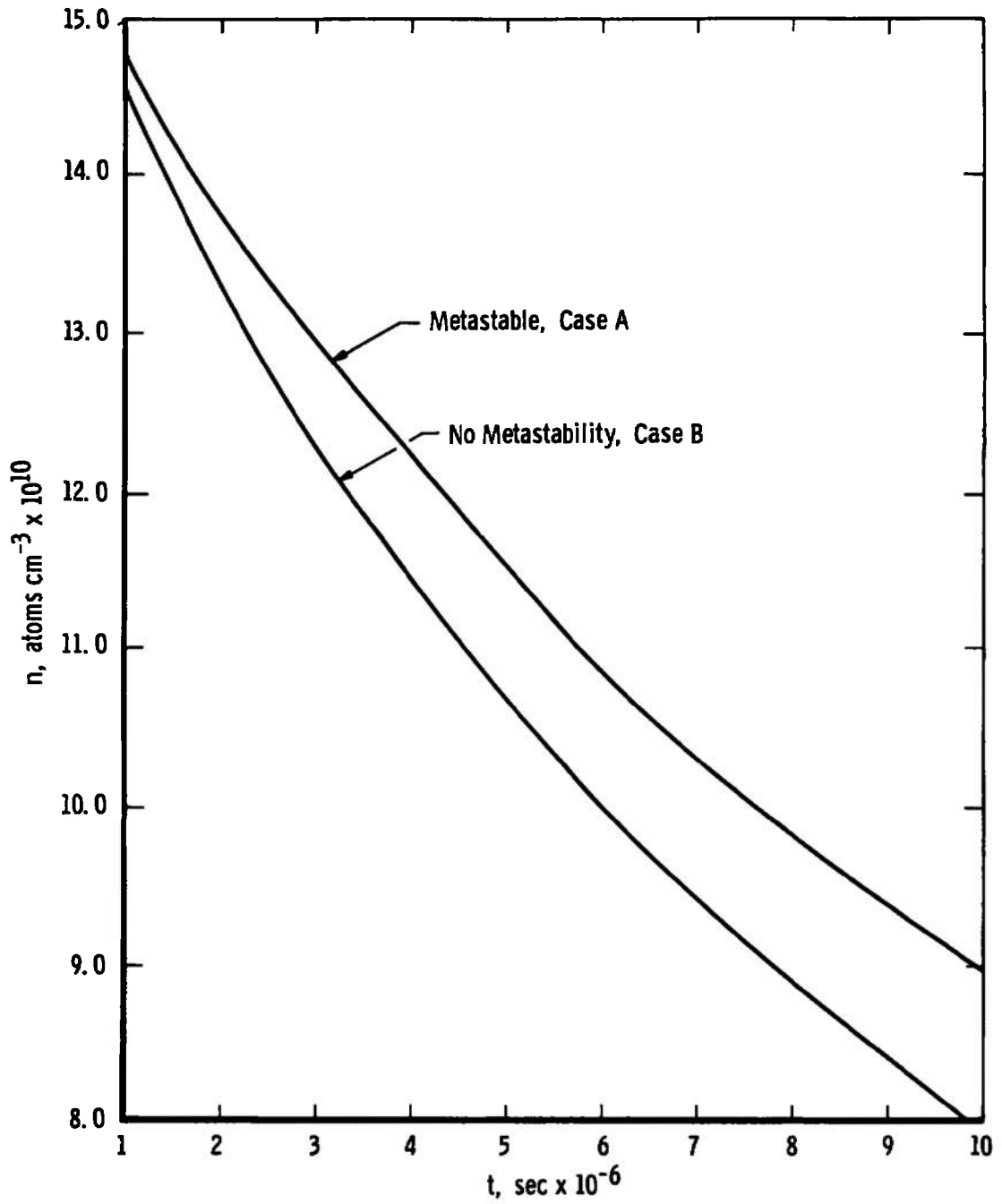


Fig. 3 Comparison of Time Developments of Quantum Level 5

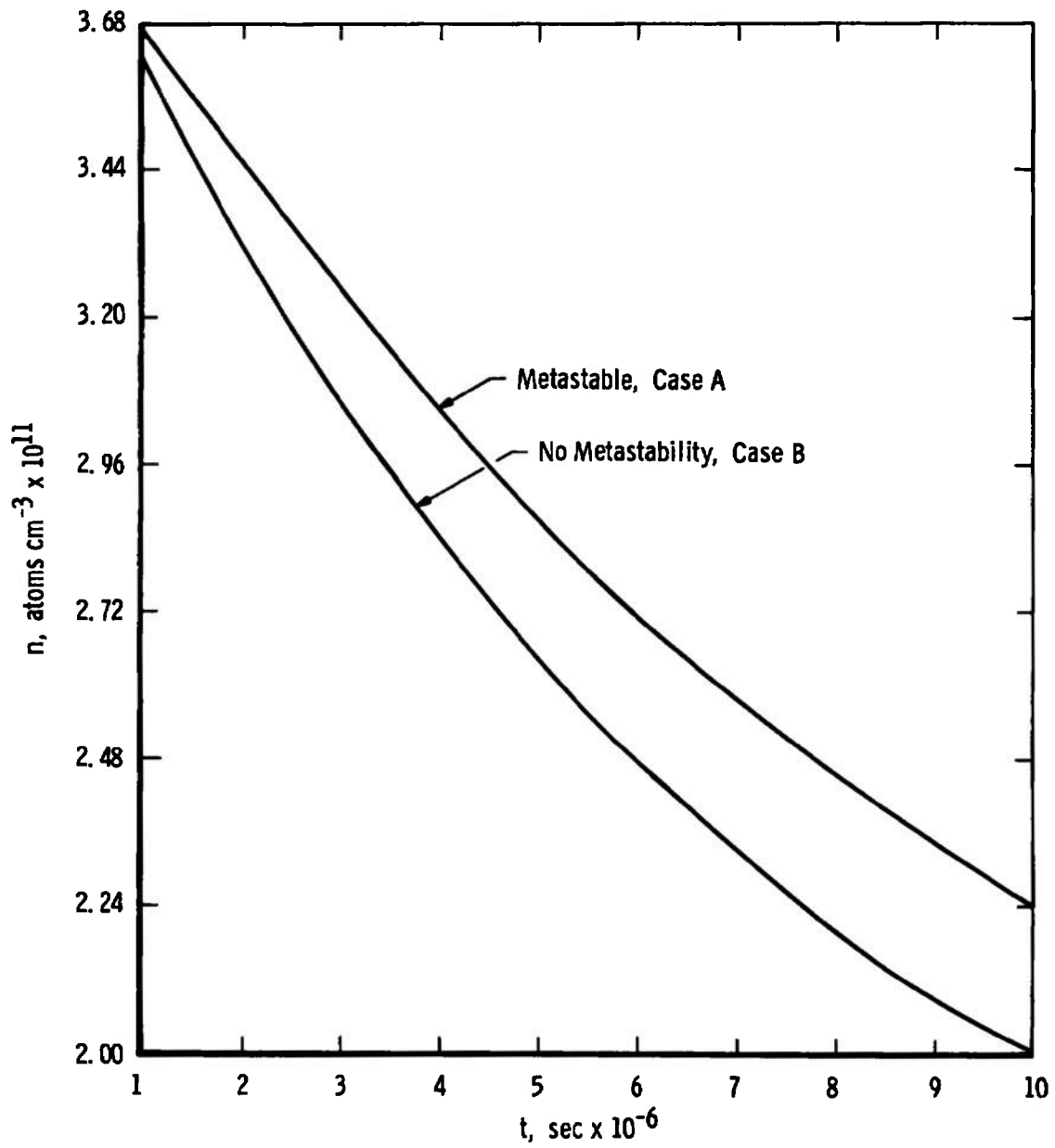


Fig. 4 Comparison of Time Developments of Quantum Level 10

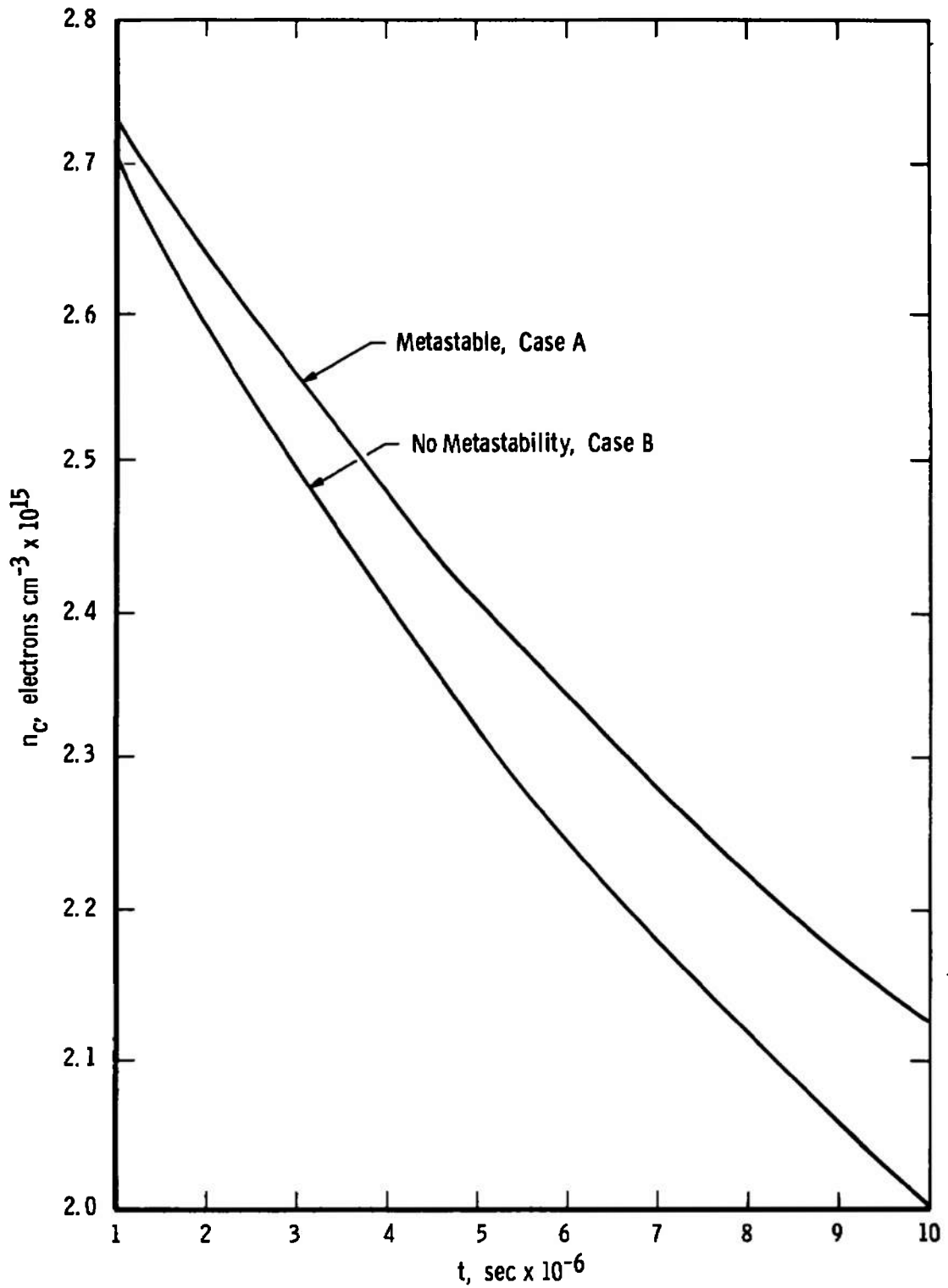


Fig. 5 Comparison of Time Developments of Continuum Densities

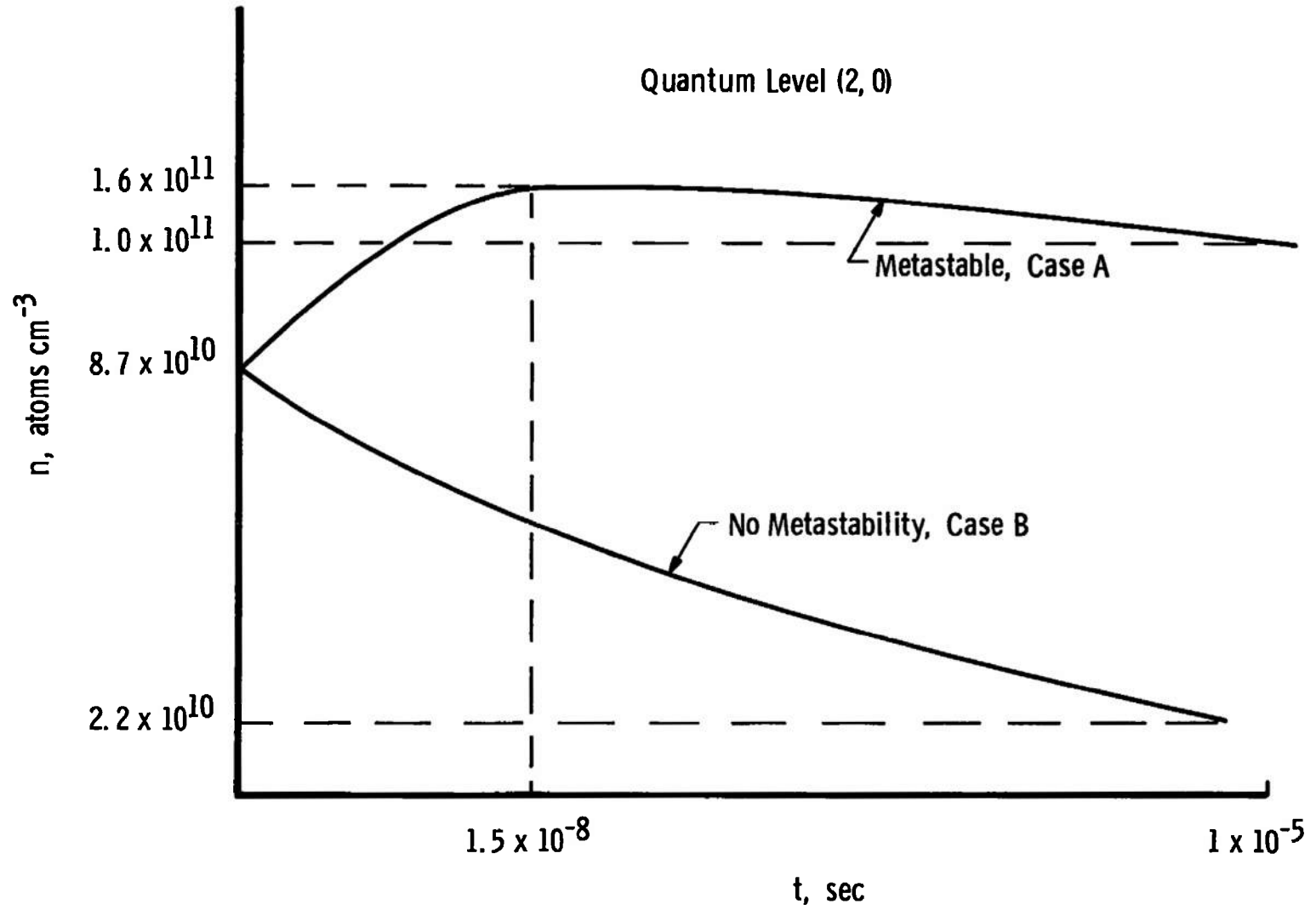


Fig. 6 Time Development of the (2,0) Population Densities

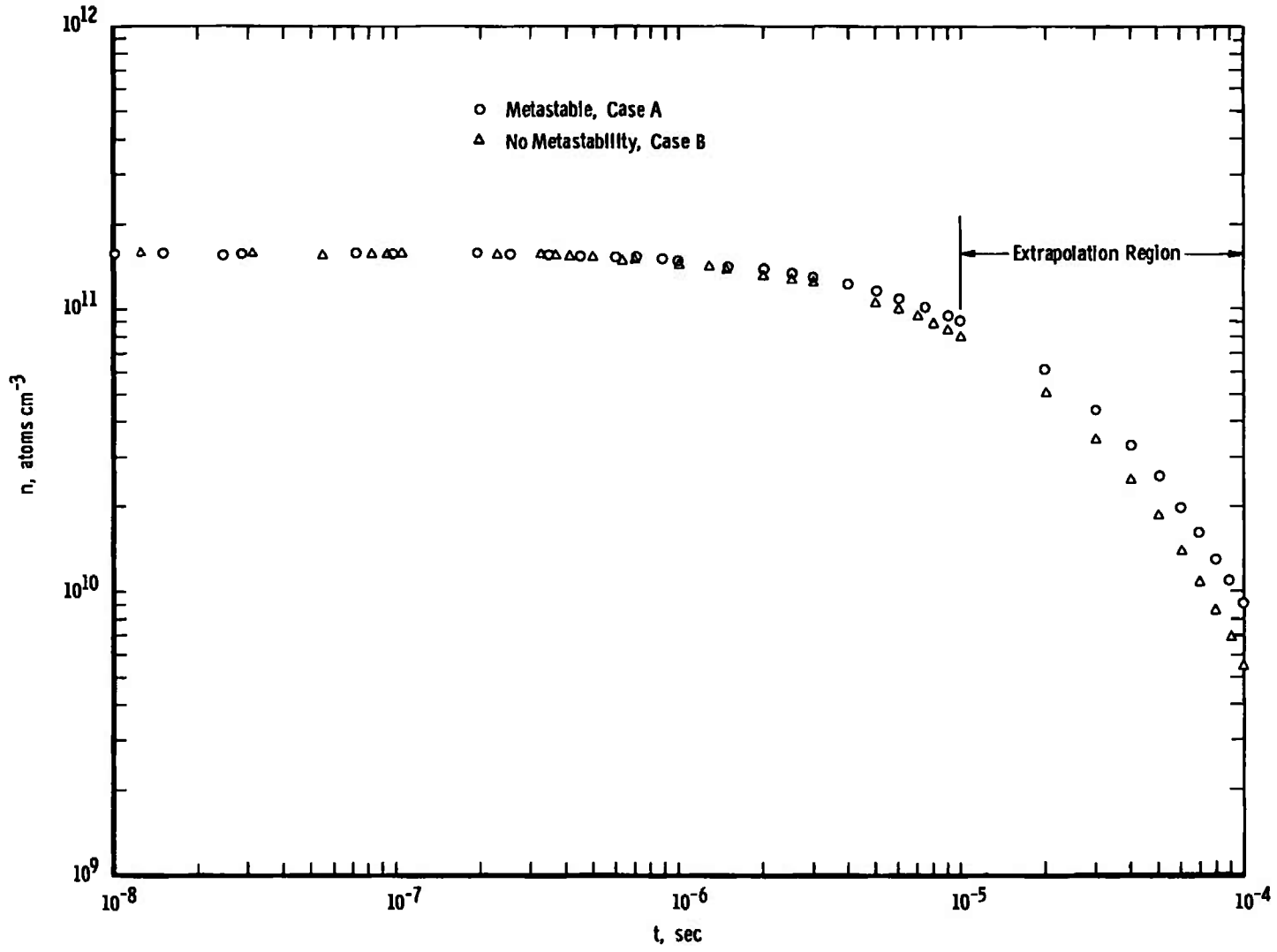


Fig. 7. Time Development of Quantum Level 5

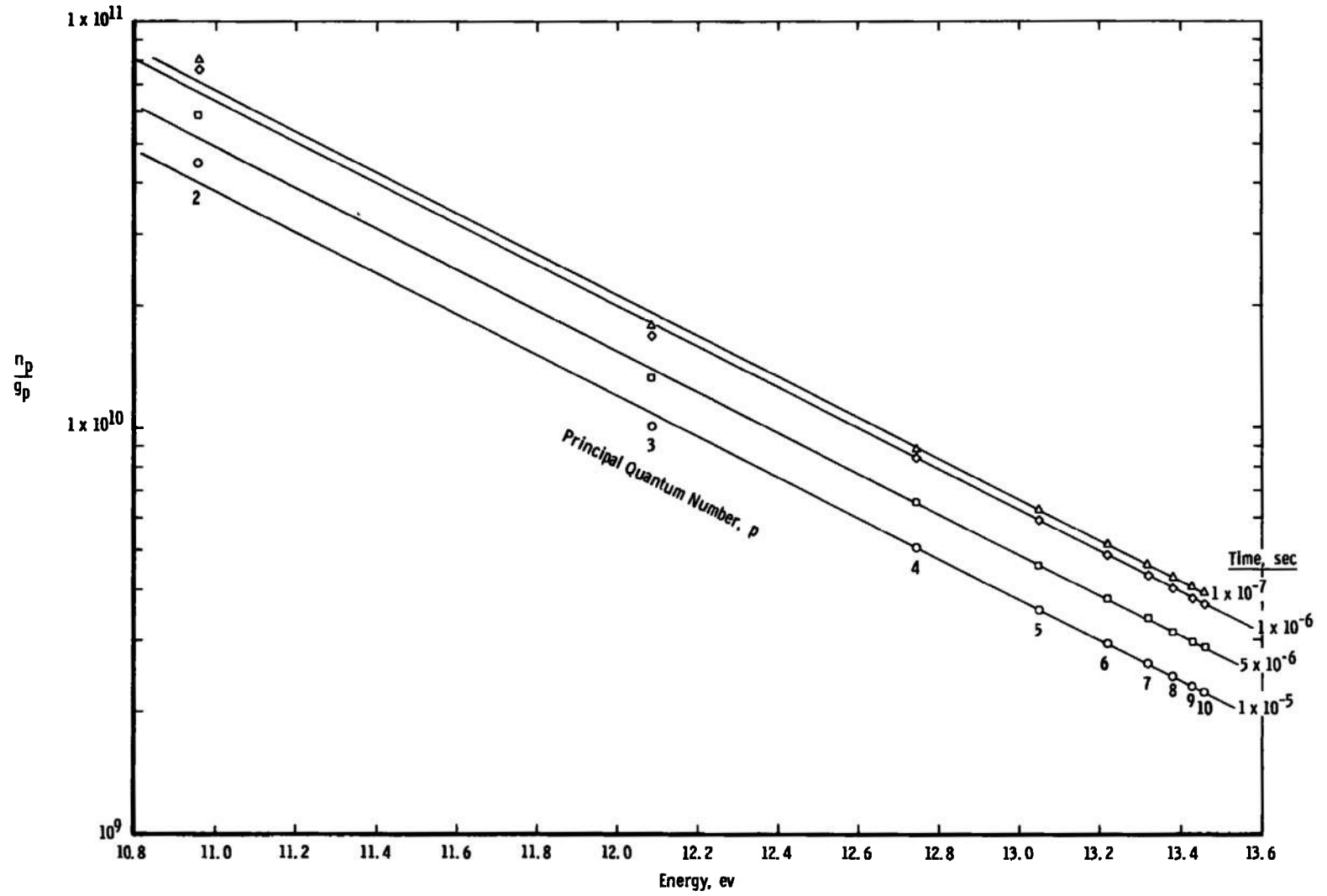


Fig. 8 Boltzmann Plot of Metastable Case A at Various Times

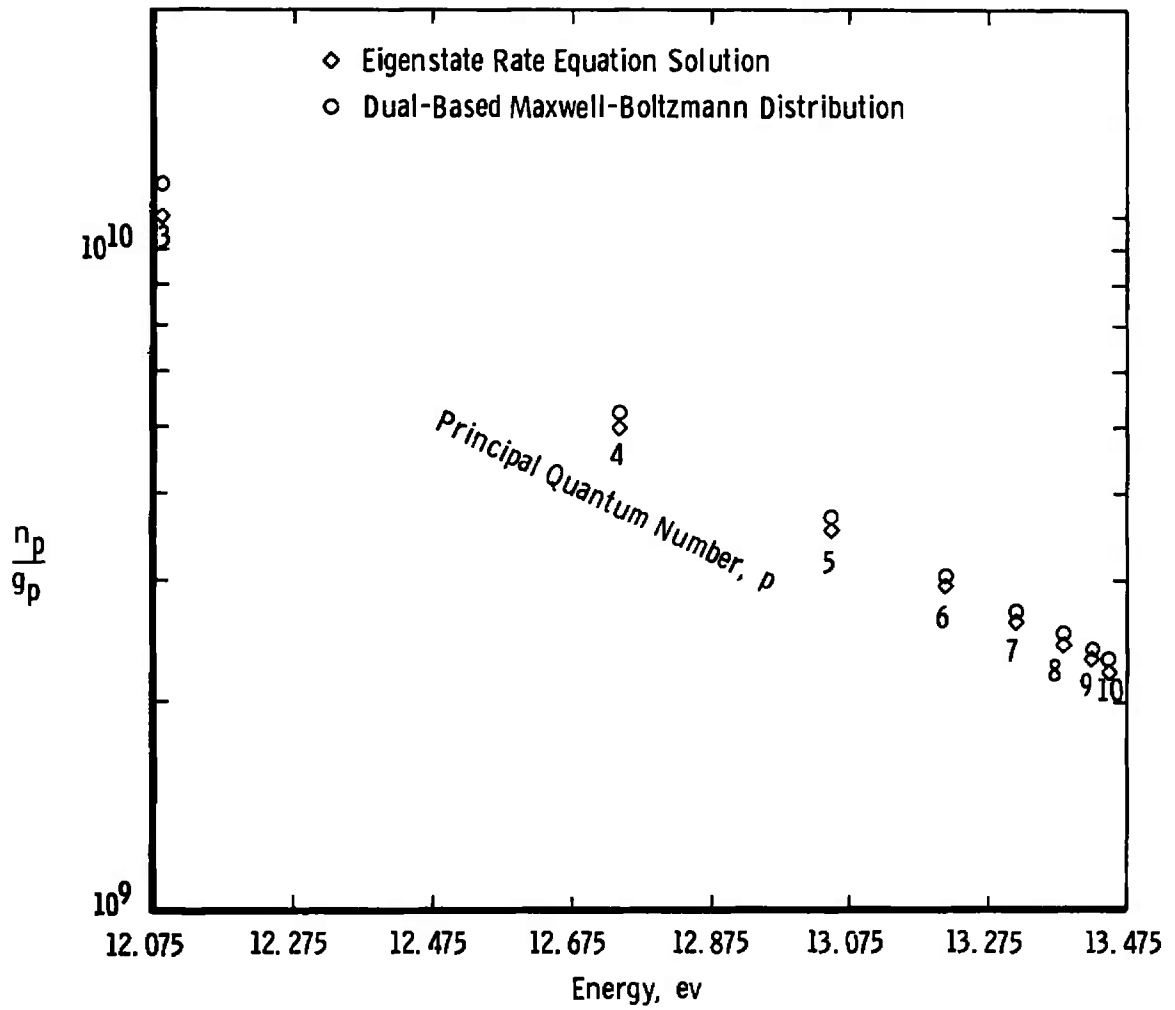


Fig. 9 Comparison of the Eigenstate Rate Equations Solution with the Dual-Based Maxwell-Boltzmann Distribution

**TABLE I**  
**RADIATIVE RECOMBINATION COEFFICIENT,  $\beta(p)$**

p	$\beta(p), \text{cm}^3 \text{sec}^{-1}$
1	$1.949 \times 10^{-13}$
2	$2.437 \times 10^{-14}$
3	$7.220 \times 10^{-15}$
4	$3.046 \times 10^{-15}$
5	$1.559 \times 10^{-15}$
6	$9.025 \times 10^{-16}$
7	$5.683 \times 10^{-16}$
8	$3.807 \times 10^{-16}$
9	$2.674 \times 10^{-16}$
10	$1.949 \times 10^{-16}$

**TABLE II**  
**TWO-BODY IONIZATION COEFFICIENT,  $K(p,c)$**

p	$K(p, c), \text{cm}^3 \text{sec}^{-1}$
1	$6.066 \times 10^{-16}$
2	$2.070 \times 10^{-9}$
3	$1.012 \times 10^{-7}$
4	$6.512 \times 10^{-7}$
5	$2.014 \times 10^{-6}$
6	$4.289 \times 10^{-6}$
7	$7.255 \times 10^{-6}$
8	$1.055 \times 10^{-5}$
9	$1.387 \times 10^{-5}$
10	$1.702 \times 10^{-5}$

TABLE III  
THREE-BODY RECOMBINATION COEFFICIENT,  $\frac{K(c,p)}{n_c}$

p	$K(c,p)/n_c, \text{ cm}^6 \text{ sec}^{-1}$
1	$1.833 \times 10^{-30}$
2	$1.800 \times 10^{-28}$
3	$2.211 \times 10^{-27}$
4	$1.174 \times 10^{-26}$
5	$3.977 \times 10^{-26}$
6	$1.005 \times 10^{-25}$
7	$2.061 \times 10^{-25}$
8	$3.631 \times 10^{-25}$
9	$5.736 \times 10^{-25}$
10	$8.369 \times 10^{-25}$

TABLE IV  
TWO-BODY INTERNAL TRANSITION COEFFICIENT,  $K(p,q)$

Q \ P	1	2	3	4	5	6	7	8	9	10
1	0	$8.711 \times 10^{-9}$	$8.031 \times 10^{-10}$	$1.705 \times 10^{-10}$	$5.318 \times 10^{-11}$	$2.082 \times 10^{-11}$	$9.481 \times 10^{-12}$	$4.814 \times 10^{-12}$	$2.653 \times 10^{-12}$	$1.559 \times 10^{-12}$
2	$2.508 \times 10^{-13}$	0	$3.076 \times 10^{-7}$	$3.661 \times 10^{-8}$	$9.311 \times 10^{-9}$	$3.302 \times 10^{-9}$	$1.422 \times 10^{-9}$	$6.970 \times 10^{-10}$	$3.752 \times 10^{-10}$	$2.168 \times 10^{-10}$
3	$5.806 \times 10^{-15}$	$7.724 \times 10^{-8}$	0	$2.402 \times 10^{-6}$	$3.048 \times 10^{-7}$	$8.364 \times 10^{-8}$	$3.167 \times 10^{-8}$	$1.441 \times 10^{-8}$	$7.391 \times 10^{-9}$	$4.133 \times 10^{-9}$
4	$1.017 \times 10^{-15}$	$7.586 \times 10^{-9}$	$1.782 \times 10^{-6}$	0	$9.332 \times 10^{-6}$	$1.274 \times 10^{-6}$	$3.716 \times 10^{-7}$	$1.463 \times 10^{-7}$	$6.887 \times 10^{-8}$	$3.641 \times 10^{-8}$
5	$3.475 \times 10^{-16}$	$2.113 \times 10^{-9}$	$2.755 \times 10^{-7}$	$1.022 \times 10^{-5}$	0	$2.122 \times 10^{-5}$	$3.517 \times 10^{-6}$	$1.083 \times 10^{-6}$	$4.451 \times 10^{-7}$	$2.163 \times 10^{-7}$
6	$1.615 \times 10^{-16}$	$8.895 \times 10^{-10}$	$8.975 \times 10^{-8}$	$1.683 \times 10^{-6}$	$2.520 \times 10^{-5}$	0	$3.455 \times 10^{-5}$	$6.835 \times 10^{-8}$	$2.296 \times 10^{-6}$	$9.948 \times 10^{-7}$
7	$8.911 \times 10^{-17}$	$4.641 \times 10^{-10}$	$4.118 \times 10^{-8}$	$5.855 \times 10^{-7}$	$5.060 \times 10^{-6}$	$4.187 \times 10^{-5}$	0	$4.685 \times 10^{-5}$	$1.067 \times 10^{-5}$	$3.882 \times 10^{-6}$
8	$5.480 \times 10^{-17}$	$2.755 \times 10^{-10}$	$2.268 \times 10^{-8}$	$2.792 \times 10^{-7}$	$1.887 \times 10^{-6}$	$1.003 \times 10^{-5}$	$5.674 \times 10^{-5}$	0	$5.731 \times 10^{-5}$	$1.453 \times 10^{-5}$
9	$3.620 \times 10^{-17}$	$1.783 \times 10^{-10}$	$1.399 \times 10^{-8}$	$1.579 \times 10^{-7}$	$9.319 \times 10^{-7}$	$4.049 \times 10^{-6}$	$1.553 \times 10^{-5}$	$6.888 \times 10^{-5}$	0	$6.598 \times 10^{-5}$
10	$2.537 \times 10^{-17}$	$1.226 \times 10^{-10}$	$9.305 \times 10^{-9}$	$9.933 \times 10^{-8}$	$5.387 \times 10^{-7}$	$2.087 \times 10^{-6}$	$6.723 \times 10^{-6}$	$2.078 \times 10^{-5}$	$7.850 \times 10^{-5}$	0

TABLE V  
TIME AT WHICH SAHA EQUILIBRIUM IS ESTABLISHED, CASE A

Quantum Number	Time, sec
10	$1.7 \times 10^{-10}$
9	$1.8 \times 10^{-10}$
8	$1.9 \times 10^{-10}$
7	$2.2 \times 10^{-10}$
6	$3.2 \times 10^{-10}$
5	$5.1 \times 10^{-10}$
4	$3.0 \times 10^{-7}$
3	_____
2	_____
1	_____

TABLE VI  
INITIAL AND FINAL POPULATION DENSITY DISTRIBUTION, CASE A

Quantum Number	Initial Population Density $\times 10^{10}$ , atoms $\text{cm}^{-3}$	Final Population Density $\times 10^{10}$ , atoms $\text{cm}^{-3}$	Final Rate $\times 10^{15}$ , atoms $\text{cm}^{-3} \text{sec}^{-1}$
1	2406740.0	2477281.0	47008.0
2,0	8.7	10.1	-276.6
2,1	26.2	7.9	-332.5
3	8.8	9.0	-27.8
4	7.3	8.0	-8.1
5	8.0	8.9	-5.8
6	9.4	10.6	-5.9
7	11.4	12.8	-6.7
8	13.9	15.5	-7.9
9	16.7	18.7	-9.5
10	19.8	22.2	-11.3
Continuum	283130.2	212595.0	-46316.0

TABLE VII  
INITIAL AND FINAL POPULATION DENSITY DISTRIBUTION, CASE B

Quantum Number	Initial Population Density $\times 10^{10}$ , atoms $\text{cm}^{-3}$	Final Population Density $\times 10^{10}$ , atoms $\text{cm}^{-3}$	Final Rate $\times 10^{15}$ , atoms $\text{cm}^{-3}/\text{sec}^{-1}$
1	2406740.0	2489118.0	51247.0
2,0	8.7	2.2	-120.1
2,1	26.2	6.8	-356.1
3	8.8	7.8	-25.9
4	7.3	7.1	-7.9
5	8.0	8.0	-5.8
6	9.4	9.4	-5.9
7	11.4	11.4	-6.8
8	13.9	13.8	-8.1
9	16.7	16.6	-9.7
10	19.8	19.8	-11.6
Continuum	283130.2	200779.0	-50689.0

TABLE VIII  
DETAILED RATES\* AT  $1 \times 10^{-15}$  SEC

Quantum Number	$T1 \times 10^{20}$ Two-Body Ionization Depopulation	$T2 \times 10^{20}$ Two-Body Internal Depopulation	$T3 \times 10^{16}$ Spontaneous Transitions Depopulation	$T4 \times 10^{20}$ Two-Body Internal Population	$T5 \times 10^{16}$ Spontaneous Transitions Population	$T6 \times 10^{20}$ Three-Body Recombination Population	$T7 \times 10^{16}$ Radiative Recombination Population
1	0.0004133	0.1760	0.0	0.008885	17087.1	0.0004161	156.26
2,0	0.005122	0.2415	0.0** 524.6	0.2631	22.22	0.01022	4.883
2,1	0.01537	0.7246	1643.5	0.7893	308.79	0.03065	14.65
3	0.2520	6.831	87.84	6.835	45.36	0.5018	5.788
4	1.3389	31.80	21.93	31.80	12.70	2.664	2.442
5	4.537	97.44	9.133	97.44	4.80	9.027	1.250
6	11.47	215.7	4.907	215.7	1.168	22.82	0.7234
7	23.52	380.75	4.236	380.8	1.070	46.77	0.4556
8	41.44	567.6	1.994	567.6	0.5366	82.41	0.3052
9	65.46	704.4	1.408	704.4	0.2344	130.18	0.2144
10	95.52	480.8	1.090	480.7	0.0	189.95	0.1563

\*Each entry expresses a time rate of change, atoms  $\text{cm}^{-3} \text{sec}^{-1}$ .

\*\*The top number is for case A and the bottom number for case B.

**TABLE IX**  
**DETAILED RATES\* AT  $5 \times 10^{-10}$  SEC**

Quantum Number	$T1 \times 10^{20}$ Two-Body Ionization Depopulation	$T2 \times 10^{20}$ Two-Body Internal Depopulation	$T3 \times 10^{17}$ Spontaneous Transitions Depopulation	$T4 \times 10^{20}$ Two-Body Internal Population	$T5 \times 10^{20}$ Spontaneous Transitions Population	$T6 \times 10^{20}$ Three-Body Recombination Population	$T7 \times 10^{16}$ Radiative Recombination Population
1	0.0004132	0.17597	0.0	0.07617	1914.8	0.0004157	156.2
2,0	0.004259	0.2008	0.0** 436.3	0.4365	39.97	0.01021	4.880
2,1	0.01272	0.5999	1361.1	1.309	559.2	0.03062	14.64
3	0.4443	12.04	154.1	12.41	88.13	0.50134	5.784
4	2.589	61.49	42.40	61.52	25.04	2.662	2.440
5	8.923	191.63	17.97	191.58	9.497	9.017	1.249
6	22.67	426.2	9.698	426.1	4.293	22.797	0.7230
7	46.55	753.7	8.388	753.5	2.1198	46.73	0.4553
8	82.08	1124.4	6.744	1124.22	1.064	82.32	0.3050
9	129.72	1395.9	2.792	1395.6	0.4648	130.0	0.2142
10	189.3	952.9	2.162	952.5	0.0	189.8	0.1562

\*Each entry expresses a time rate of change, atoms  $\text{cm}^{-3} \text{sec}^{-1}$ .

\*\*The top number is for case A and the bottom number for case B.

**TABLE X**  
**DETAILED RATES\* AT  $1 \times 10^{-5}$  SEC**

Quantum Number And Case	T1 x 10 <sup>19</sup> Two-Body Ionization Depopulation	T2 x 10 <sup>20</sup> Two-Body Internal Depopulation	T3 x 10 <sup>17</sup> Spontaneous Transitions Depopulation	T4 x 10 <sup>20</sup> Two-Body Internal Population	T5 x 10 <sup>17</sup> Spontaneous Transitions Population	T6 x 10 <sup>19</sup> Three-Body Recombination Population	T7 x 10 <sup>14</sup> Radiative Recombination Population
1 A	0.00319	0.136050	0.0	0.035352	562.1069	0.00176	8810.3
1 B	0.00303	0.129102	0.0	0.174086	616.4612	0.00148	7858.2
2,0 A	0.04441	0.209432	0.0	0.204209	2.2075	0.04324	275.3
2,0 B	0.00929	0.043814	134.1824	0.171833	2.0024	0.03643	245.6
2,1 A	0.03473	0.163806	494.8042	0.612629	32.3293	0.12974	825.9
2,1 B	0.02808	0.132451	423.6390	0.515501	28.1709	0.10928	736.7
3 A	1.93794	5.352209	89.3109	5.317253	4.9156	2.12458	326.3
3 B	1.58493	4.295474	77.3088	4.347325	4.4371	1.78963	291.0
4 A	11.04610	26.233615	24.0793	26.232723	1.4154	11.27947	137.6
4 B	9.24707	21.961066	21.3432	21.955530	1.2602	9.50124	122.7
5 A	37.91466	81.424734	10.1623	81.404279	0.5364	38.21418	70.5
5 B	31.86433	68.431175	9.0432	68.407089	0.4780	32.18964	62.8
6 A	96.20751	180.879494	5.4794	180.844591	0.2424	96.60791	40.8
6 B	80.94325	152.181212	4.8814	152.142358	0.2160	81.37749	36.4
7 A	197.47552	319.703919	4.7370	319.653880	0.1196	198.02116	25.6
7 B	166.21158	269.089021	4.2217	269.033928	0.1067	166.80375	22.9
8 A	348.12996	476.894613	2.2315	476.822421	0.0600	348.87261	17.2
8 B	293.06771	401.466204	1.9891	401.387595	0.0535	293.87219	15.3
9 A	550.12175	591.962841	1.5761	591.864326	0.0262	551.12134	12.1
9 B	463.15336	498.379819	1.4050	498.272825	0.0234	464.23603	10.8
10 A	802.81945	404.082342	1.2205	403.951388	0.0	804.13997	8.8
10 B	675.93561	340.218022	1.0880	340.075967	0.0	677.36581	7.8

\*Each entry expresses a time rate of change, atoms cm<sup>-3</sup> sec<sup>-1</sup>.

**TABLE XI**  
**COMPARISON OF THE EIGENSTATE RATE EQUATION SOLUTION WITH THE**  
**DUAL-BASED MAXWELL-BOLTZMANN DISTRIBUTION**

Quantum Number	$n_p/g_p$ Eigenstate Rate Equation	$n_p/g_p$ First Maxwell Boltzmann	$n_p/g_p$ Second Maxwell Boltzmann	$n_p/g_p$ First + Second	Percentage Deviation
1	$2.4773 \times 10^{16}$	$2.4773 \times 10^{16}$	0.0	$2.4773 \times 10^{16}$	0.0
2,0	$1.0096 \times 10^{11}$	$8.9990 \times 10^{10}$	$1.0966 \times 10^{10}$	$1.0096 \times 10^{11}$	0.0
2,1	$2.6320 \times 10^{10}$	$8.9990 \times 10^{10}$	$1.0966 \times 10^{10}$	$1.0096 \times 10^{11}$	285.0
3	$1.0007 \times 10^{10}$	$1.0059 \times 10^{10}$	$1.226 \times 10^9$	$1.1285 \times 10^{10}$	12.77
4	$4.9871 \times 10^9$	$4.6719 \times 10^9$	$5.963 \times 10^8$	$5.2412 \times 10^9$	5.1
5	$3.5418 \times 10^9$	$3.2759 \times 10^9$	$3.992 \times 10^8$	$3.6751 \times 10^9$	3.8
6	$2.9311 \times 10^9$	$2.7014 \times 10^9$	$3.292 \times 10^8$	$3.0306 \times 10^9$	3.4
7	$2.6128 \times 10^9$	$2.4049 \times 10^9$	$2.930 \times 10^8$	$2.6979 \times 10^9$	3.3
8	$2.4245 \times 10^9$	$2.2301 \times 10^9$	$2.717 \times 10^8$	$2.5018 \times 10^9$	3.2
9	$2.3026 \times 10^9$	$2.1176 \times 10^9$	$2.580 \times 10^8$	$2.3757 \times 10^9$	3.2
10	$2.2193 \times 10^9$	$2.0404 \times 10^9$	$2.487 \times 10^8$	$2.2894 \times 10^9$	3.2

## DOCUMENT CONTROL DATA - R &amp; D

*(Security classification of title, body of abstract and indexing annotation must be entered when the overall report is classified)*

1. ORIGINATING ACTIVITY (Corporate author) Arnold Engineering Development Center ARO, Inc., Operating Contractor Arnold Air Force Station, Tennessee 37389		2a. REPORT SECURITY CLASSIFICATION UNCLASSIFIED	
		2b. GROUP N/A	
3. REPORT TITLE NUMERICAL STUDY OF THE EARLY POPULATION DENSITY RELAXATION OF THERMAL HYDROGEN PLASMAS			
4. DESCRIPTIVE NOTES (Type of report and inclusive dates) Final Report July 1, 1968 to March 1, 1969			
5. AUTHOR(S) (First name, middle initial, last name) C. C. Limbaugh and W. K. McGregor, Jr., ARO, Inc., and A. A. Mason, The University of Tennessee Space Institute			
6. REPORT DATE October 1969	7a. TOTAL NO. OF PAGES 59	7b. NO. OF REFS 19	
8a. CONTRACT OR GRANT NO F40600-69-C-0001	9a. ORIGINATOR'S REPORT NUMBER(S) AEDC-TR-69-156		
b. PROJECT NO. 8951	9b. OTHER REPORT NO(S) (Any other numbers that may be assigned this report) N/A		
c. Task 05			
d. Program Element 61102F			
10. DISTRIBUTION STATEMENT This document has been approved for public release and sale; its distribution is unlimited.			
11. SUPPLEMENTARY NOTES Available in DDC.		12. SPONSORING MILITARY ACTIVITY Arnold Engineering Development Center, Air Force Systems Command, Arnold AF Station, Tenn. 37389	
13. ABSTRACT The purpose of this investigation was to examine the early relaxation of the population density distribution of a thermal hydrogen plasma. The system of rate equations describing the transient behavior of all quantum levels was used and solved numerically. Three hypothetical hydrogen plasmas were studied, each with an excitation temperature of 10,000°K. Two of the plasmas differed only by the transition probability of the quasi-metastable $2S_{1/2}$ eigenstate, whereas the third case used a different initial population density distribution. The plasmas were used to study the fundamental consistency of the mathematical model, the existence and location of the critical level, relaxation to the quasi-steady state, and a quantitative study of the effects of the quasi-metastable level on the excited state population density distribution. The results show that the model is consistent with fundamental theory under strong collision dominance and that the critical level does exist at that level predicted by earlier investigators.			

14. KEY WORDS	LINK A		LINK B		LINK C	
	ROLE	WT	ROLE	WT	ROLE	WT
plasma density						
Maxwell-Boltzmann equation						
hydrogen plasmas						
quantum statistics						
electron distribution						
excitation						
1 Hydrogen Plasmas						
2 Plasmas - Distribution, Excitation						
3 Electrons - Density						
4 " - Distribution						
5 - 25						